Spectrum of Engineering Sciences
ISSN (e) 3007-3138 (p) 3007-312X Volume 4, Issue 5, 2026

SPATIO-TEMPORAL ANALYSIS OF LAND USE/LAND COVER DYNAMICS AND ITS IMPACT ON LAND SURFACE TEMPERATURE USING GEOSPATIAL TECHNIQUES: A CASE STUDY OF MARDAN, PAKISTAN

Umair Aftab Choudary[1], Attiq Ur Rahman Faridi[2], Maryam Khalid[3], Ayesha Javed[4], Manzer Javed Sindhu[5], Muhammad Ishfaq[*6], Sobia Rani[7]

[1]*MS Scholar, Bahria University, Islamabad*
[2]*Department of Geography, University of Punjab Lahore*
[3]*Lecturer, Institute of Geography, University of the Punjab, Lahore Pakistan*
[4,5]*Institute of Geology, University of the Punjab, Lahore*
[*6]*MS Scholar, Department of Meteorology (RS and GIS), COMSATS University Islamabad*
[7]*MS Scholar, RS and GIS, Arid Agriculture University Rawalpindi*

[1]umair7906@gmail.com, [2]attiqfaridi@yahoo.com, [3]maryamkhalid.geog@pu.edu.pk, [4]aysh.javed03@gmail.com, [5]manzer.javed78@gmail.com, [*6]ishfaqgeo.gis@gmail.com, [7]sobiarani853@gmail.com

DOI: https://doi.org/10.5281/zenodo.20033604

Keywords
Spatio-temporal analysis, Land Use/Land Cover (LULC), Land Surface Temperature (LST, Remote Sensing and GIS, Urbanization, Environmental change.

Article History
Received: 11 March 2026
Accepted: 21 April 2026
Published: 05 May 2026

Corresponding Author: *
Muhammad Ishfaq

ABSTRACT

Urbanization is presently a worldwide phenomenon. Pakistan, like many other South Asian nations, is experiencing rapid urbanization, with an annual growth rate of 3%. The consequences of urbanization on the climate and environment are critical for the country's natural resource management. One of the most significant aspects of land use change is the relationship between urbanization and the decrease of agriculture as a result of increased economic growth. Furthermore, analyzing dynamic changes in land use is necessary for developing a model for future land use changes. The research examines the city of Mardan's projected land use and land use development for the year 2050. Landsat pictures for the years 1990, 2000, 2010, and 2022 were used in this study. The photos were used to determine the temperature of the earth's surface, recover land use changes in land cover, and derive indices such as NDVI, NDBaI, NDBI, UI, and NDWI. Changes can be seen in built-up regions and agricultural areas, but water bodies and uncultivated places are also affected. Agriculture accounted for 51% of GDP in 1990 and will drop to 40% by 2022. From 1990 to 2022, the Built-up increased from 0.97 percent to 8.01 percent. The total accuracy of the images was between 89 and 90 percent. The LULC model has a significant impact on the projected temperature fluctuation. Additionally, a probability transition image was produced using the Markov model, demonstrating the transition forecast in the LULC model up to 2050, which shows a 35 percent decline in agricultural and a 136 sq.km rise in buildings. LST can be used to reflect the effect of a transition in the LULC model. The average maximum temperature in 1990 was 40 degrees Celsius, rising to 46 degrees Celsius in 2022, according to seven separate yearly photos acquired by the LANDSAT thermal band. LST was analyzed using linear regression with NDVI, NDBI, NDWI, UI and NDBaI. The study found that NDVI had a negative relationship with LST. LST rises when plant cover decreases. While LST has a high positive connection *with NDBI, NDBaI, UI and NDWI. As a result, immediate steps must be taken to limit the rapid disappearance of urbanization in order to minimize environmental, natural resource, and biodiversity devastation by managing the evolution of soil surface temperature.*

INTRODUCTION

Urbanization results in the displacement of natural land cover with grey constructions, which alters the biophysical climate of the city and the Land surface temperature (LST). The surface energy and radiation balance were disrupted when natural surfaces were converted to impermeable surfaces, resulting in a low heat exchange capability. The urban heat island effect (UHI) arises as a result of the modification of land surfaces, infrastructural materials, and the emission of heat from human activities.

Currently, the world's most energy–intensive locations are Asia's metropolitan areas, where the rapidly expanding urban sprawl with a big population, acute energy shortages, and intensive urban infrastructure have a significant impact on the current level of city inhabitants. It also influences the urban environment and climate (Ren *et al.*, 2012). Climate scientists that have examined indigenous and regional climates under human impact have been paying close attention to the fast shift in the climate's driving features over the last decade. Global climate change is exacerbated by rapidly rising industrialization and development. The increase in LST caused by the decline in agricultural land and the growth of hard, impenetrable, and non–evaporative sides is currently the major challenge of metropolitan regions. Because of the more visible consequences of changes in terrestrial ecosystems owing to human activities, land use / land cover change (LULC) has had an impact on the environment locally, regionally, and globally. Because vegetation is one of the primary producers of humidity, the shift from natural to urbanized regions has a significant impact on the quantity of humidity in the air (Ibrahim, 2017).

Urbanization refers to the increase in human population in some places as well as the conversion of land for residential, commercial, industrial, and transportation reasons. The urban population has expanded at an unparalleled rate in the twenty–first century, from 30% in 1950 to 54 percent in 2014, and is expected to grow by 66 percent by 2030, with estimates that by 2050, 64 percent and 56 percent of the population would be urban. Traffic congestion, infrastructure growth, and the availability of basic requirements like as water, wastewater, and power have all presented severe challenges to urban planners. Other impacts include habitat loss and the establishment of heat islands as a result of human–caused heat emission, as well as a decline in permeable surfaces and flora. The interiors of cities are cooler than the suburbs of densely populated places. An urban heat island is defined as a significant temperature variation in one location compared to another (UHI). Numerous satellite data have employed electromagnetic spectrum products in the thermal sector to research the UHI phenomena using satellite measurements of the Earth's surface temperature to investigate the problem (LST). Most major cities across the world are familiar with UHI. The temperature at the soil surface is very important for assessing surface heat islands. The temperature of the soil's surface can also be used to study plant function (Franco et al., 2015) . The majority of natural vegetation has been converted to urbanization across the world (Hepcan *et al.*, 2013). Due to the high rise of urban sprawl, a loss in plant cover and a matching increase in impervious areas typically leads to an intense conversion of the city's surface structure, materiality, and spatial distribution. Such variations produce a redistribution of received solar radiation and air temperature, resulting in a differential in surface radiation between urban and rural areas (Zhao *et al.*, 2016).

Urbanization is the most widespread human activity that results in agricultural loss, environmental extinction, and a decline in natural plant cover. In recent human history, the development change from rural to urban proportions has been disproportionately large, with significant implications for the natural functioning of living environments. Metropolitan areas make up just 3% of the earth's surface, yet they have a considerable influence on climate change and environmental conditions both worldwide and locally. In urban regions, human activities have a significant influence on the environment, and the conversion of urban land use and land cover (LULC) is considerably more deliberate. The geographical properties of LULC are valuable for understanding the varied effects of human activities on ecological disturbances in the urban environment, hence such studies are becoming more important. Anthropogenic activities are occurring quicker in developing nations as a result of LULC change, and it is anticipated that by 2020, the majority of the world's megacities will be in developing countries, a driver of rapid LULC change and greater ecological degradation. Because the world's urban population is expected to treble by 2050, population influence will be very crucial (Lelieveld *et al.*, 2015).

Rapid urbanization, which has resulted in a significant reduction in vegetative cover and, as a result, an increase in impermeable area, has resulted in an enormous growth in people and infrastructure in cities. The urban heat island that forms in the city's core radiates more than the surrounding surroundings (Ma *et al.*, 2010). To monitor urban growth and the urban environment, better development methodologies and structures are required. Furthermore, data collected with time resolution, as well as various spectral, spatial, and angular data, have been used to investigate land cover changes associated with urban sprawl in recent years, as well as to retrieve biophysical considerations of the earth's surface, such as surface temperature, opulence of plantations, and built indices, which are a good indicator of the state of the urban environment (Ma *et al.*, 2010).

Many experts from all around the globe have researched the impact of urbanization on atmospheric qualities in various cities during the last two decades (Fu and Weng, 2018).

By 2030, it is expected that 81 percent of the world's population will be urban. As the global urbanization process expands in terms of area and volume, there is a rising interest in how it is linked to a variety of environmental factors such as biodiversity, climate, and weather on a local, global, and regional scale (Imhoff *et al.*, 2010). Long-term climatic changes are affecting the Earth's surface temperature as a result of urban development and accompanying activities (LST). Solar radiation absorption, energy storage, evaporation, surface temperature, and air changes around cities are all factors to consider. The vegetative cover around and in metropolitan areas gradually turns into a solid and impermeable surface, resulting in an increase in LST (Vani and Prasad, 2020).

Infrared thermal remote sensing may be used to get the Earth's surface temperature (LST), which is a well-known indication of surface UHI (Wang *et al.*, 2018). Changes in land cover can be divided into two categories. Moving land cover from one group to another is one sort of transition. Meadows emerge from the forest. Although the group remains the same, the other sort of change is to reform the environmental qualities of land usage by human activities or natural practices. Land use change is an example of forest degradation caused by erosion activities (Powell and Roberts, 2010). The alteration of land and atmosphere that occurs as a result of the establishment and administration of cities is incredible. Changes in land form, as well as surface material connected with infrastructure, alter air currents, which act as water and energy replacements. A tranquil urban climate is created by the direct emission of heat, pollution, and carbon dioxide, as well as human activity (Kabisch *et al.*, 2019)

(UHI) is the most important micro-scale climate change phenomena. A heat island is defined as the thermal differential between one location with a high temperature and another location with a lower temperature. There are UHIs in urban regions where the air temperature is greater than in rural ones (Şahin *et al.*, 2012). LST is a demanding constraint in the International Geosphere and Biosphere Program, and it is also widely employed in many fields such as the water cycle, land cover monitoring, evapotranspiration, Green cover, unlike an impermeable surface, has an influence on cold lands through evaporation and emissivity, as well as decreased thermal inactivity, hence a drop in LST can occur as a result of an increase in green cover (Estoque *et al.*, 2017). Land use and cover is acknowledged as one of the most essential aspects of environmental transition at the global and regional levels. The major LULC conversion process is the multifaceted relationship between human activities and the environment (Shiferaw and Singh, 2011). Thermal data characteristics and quality are vital to planners and urban planners in order to increase the quality of urban environments and make them more ecologically friendly. Soil surface temperature and emissivity are crucial variables in determining the energy balance when considering land usage (Chakraborty *et al.*, 2015).

The Geographic Information System (GIS), remote sensing, and the creation of a decision support system for Earth's Surface Temperature (LST) and other ecological techniques were considered as extremely accessible and useful instruments (Shekhar and Pandey, 2015) Remote sensing and Geographic Information Systems (GIS) have long been significant tools for tracking and evaluating changes in urban land use and land cover. Satellite remote sensing integrates multi–resolution, multi–temporal, and multi–spectral data and translates it into relevant information to detect and analyse urban soil treatments and urban land cover data sets (Zhang and Lin, 2019). The Advanced Very High–Resolution Radiometric System (AVHRS) of the National Oceanic and Atmospheric Administration (NOAA) was used to acquire LST satellite remote sensing data for metropolitan areas (AVHRR).

1.2 Land Use–Land Cover and UHI in Pakistan

Over time, there is a sharp increase in urbanization in Pakistan, which transforms the internal structure of land use. Pakistan lacks future urban planning, which is the essential part of urban planning for land use changes(Mehmood *et al.*, 2017) For least developed countries like climate change, and ecological research (Li *et al.*, 2013).

Pakistan, one of the crucial problems is unsystematic changes in land cover, which lack adequate development techniques. There are several methods by which land use changes disrupt the urban environment, such as the production of pollutants by human activities, local climate change, marginalization and the destruction of natural habitats. The spatial configuration of the landscape is expected to influence environmental processes (Hassan *et al.*, 2016a)

Seasonal fluctuations, mountain ranges, and plains are all part of Pakistan's geographic and climatic trends. The climate of the nation may be defined as dry, with scorching summers and chilly winters with varied amounts of humidity. However, it has long been recognized that rising temperatures and humidity as a result of climate change constitute a serious weather threat. The country's high heat indices indicate a climate problem (Khan *et al.*, 2019). The rise in the heat index is related to Urban Heat Island (UHI), a phenomenon in which the temperature in a metropolitan region is greater than in nearby less developed rural areas. The "ability of the surfaces of each environment to absorb and store heat" determines the temperature differential between rural and urban locations. Heat is created in metropolitan areas mostly as a result of increasing human activity and the usage of automobiles, both of which emit excessive quantities of energy into the atmosphere. Furthermore, industrial buildings are constructed in close proximity to one another, and the materials used to construct them effectively insulate or retain heat (Khan *et al.*, 2020).

According to heat index data, Pakistan has experienced a considerable rise in temperature in recent decades. Changes in plant cover are the primary consequence of UHI. May is the commencement of the extreme weather season, which lasts until September. A heat wave has reached parts of the country, with maximum temperatures exceeding 45 degrees Celsius (Khan *et al.*, 2019).

1.3 Role of GIS/RS in Land Use–Land Cover and Urban Heat Island

Land use and land cover in the region are disrupted by disorganized urbanization and urban sprawl. Due to the residential area, land use change includes land use due to decreasing cultivated land, decreasing forests, increasing non-productive land and impermeable surfaces. Regional land use planning benefits city dwellers and policy makers (Tan *et al.*, 2010).

The decisive consequence of urban expansion is the escalation of the surface temperature and the emergence of urban heat islands. The heat given off by human activities due to the use of energy increases the surface temperature, the synthetic material has a high thermal capacity and conductivity, which increases the exposure of the earth's surface, the associated reduction of vegetation cover and the permeable surface to water due to evapotranspiration. Decrease the surface temperature. Landsat ETMs are widely used to monitor and visualize the biophysical properties of the earth's surface. Furthermore, Landsat Imagery is suitable for capturing surface temperature and creating land cover maps. Landsat TM River Delta were investigated (Muster *et al.*, 2012).

LULC change owing to urbanization is one of the most significant anthropogenic effects on urban climate, and it has a direct impact on soil surface temperature (LST). However, the impact of LULC alterations on LST and the urban heat island (UHI) has yet to be investigated. Using satellite remote sensing data, we evaluated the LULC variations in Islamabad from 1993 to 2018, their warming (positive) and cooling (negative) impacts, and their contribution to the associated LST (RLST). A random forest classifier (RF) was used to classify the LULC, and a standardized radiation transfer equation was used to calculate the LST (RTE). The expense of eliminating wastelands, woodlands, meadows / cropland, and water bodies has raised impermeable surfaces by 11.9 percent over the last 26 years, according to the findings (Afshan et al., n.d.). Woodlands, water bodies, and grassland / agricultural regions that were transformed to impermeable areas contributed to the warming impacts, resulting in a 1.52° C warming contribution. Replacing parched soils and impermeable surfaces with trees and water bodies, on the other hand, can contribute 0.85° C to the RLST cooling. The conversion of forests to impermeable soils contributed 1% to the LULC differences, according to the established scale (10%), compared to a subsequent conversion of 0.2 percent (Khan et al., 2020). The positive (warmer) impact of human activities to UHI was larger than the negative (cooler) effect of changing a natural surface to an artificial surface. The data will aid city managers and land use decision-makers in regulating rising surface temperatures for acceptable living conditions and sustainable cities (Afshan *et al.*, n.d.).

The goal of this study is to examine the dynamics of LU/LC and to predict the earth's surface temperature using the indices stated above from 1990 to 2022, as well as to identify future projections for the study region in 2050.

1.4 Problem Statement

Anthropogenic activities and the relocation of populations to urban areas have caused climate change and other natural risks in the last few decades. The study region experiences a pleasant climate in winter, autumn, and spring, but summer is extremely hot and dry. According to the 2017 census, the district has a total population of 358,604 people. Due to urbanization and population growth, the city has become a hub of commercial, residential, and industrial activities. However, improper government planning and unchecked urban expansion have led to serious threats to the thermal environment in the study region. Variations in land use/land cover dynamics have caused the development of the Urban Heat Island (UHI) effect. Therefore, adequate management measures need to be implemented to reduce these risks.

1.5 Objectives

- To assess the urban heat island effect by calculating LST from thermal infrared (TIR) bands and evaluating its relationship with LULC changes.
- To evaluate the changes in LULC in the study area from 1990 to 2021.

- To analyze the relationship between different indices and LST.
- To use the research findings for long-term planning and decision-making purposes.

Data And Methodology

2.1 Study Area

The study will conduct in Mardan District, situated in Khyber Pakhtunkhwa Province, Pakistan. It is the 2nd biggest city in Khyber Pakhtunkhwa and is located in Peshawar Valley. The city has experienced rapid population growth in the latter half of the 20th century. Mardan District is bordered by Swabi district to the east, Charsadda district to the west, Malakand district to the northwest, Buner district to the northeast, and Nowshehra district to the south as shown in figure 1. The district's geographical coordinates are between latitudes 34°05'N and 34°31'N and longitudes 72°26'E and 71°49'E.

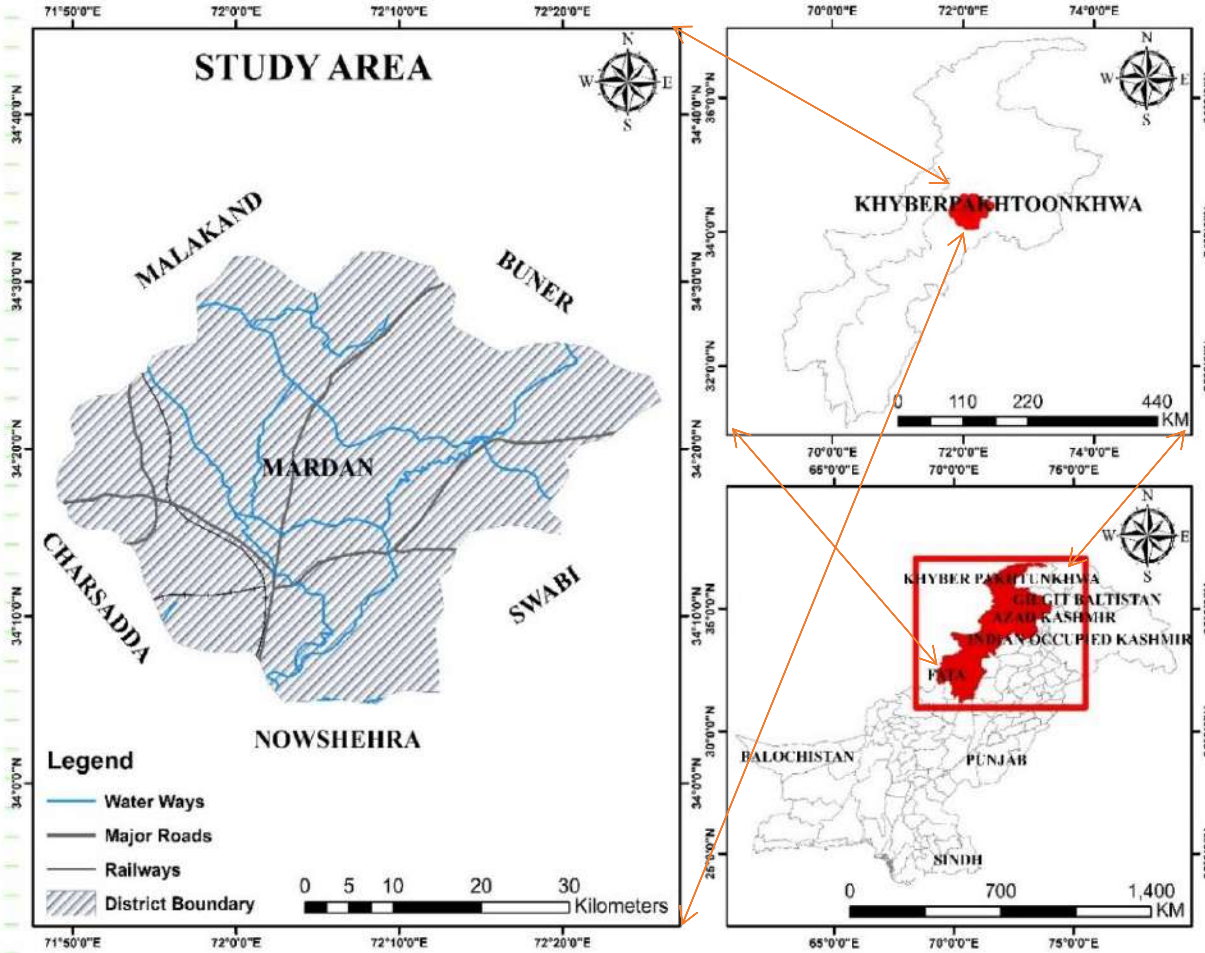

Figure 2.1 Map Showing Study Area Map of District Mardan

2.2 Data Collection

Data will be acquired through two methods: primary method and secondary method.

2.2.1 Primary Data

Landsat imagery (5, 7 and 8) of 1990, 2000, 2010 and 2022 will be collected from the (USGS) United States Geological Survey website. Data will be collected at various locations throughout the study area for accuracy assessment through GPS.

2.2.2 Secondary Data

Various sources and government agencies will provide secondary data to achieve the research goals. The Department of Planning and Development Mardan, Khyber Pakhtunkhwa will provide the shapefile of the study area.

2.3 Data Processing

The data processing is discussed below also shown in flow chart (Fig.2).

2.3.1 Image Analysis

Land use and land cover (LULC) classification is crucial to identify changes in LULC over the study area defined time period. Four categories, including vegetation, settlement, barren land, and water body, will be used to group the photographs. Natural color composites from each year will be utilized to categorize the imagery. The maximum likelihood classifier combined with supervised signature extraction will be used to categorize Landsat photos. The classifier will receive about 200 training samples from the image for the following classes: Vegetation, Settlement, Bare Land, and Water Body. The accuracy of each image will then be evaluated, and the area will be calculated.

2.3.2 Normalized Difference Vegetation Index (NDVI)

The Normalized Differential Vegetation Index (NDVI) is used to evaluate whether or not the captured objective reality contains green vegetation and is a key indicator of the built environment (Li and Liu, 2008). NIR and Red Band of Landsat satellite Images will be used for this research. It can be calculated as:

NDVI=(NIR–RED)/(NIR+RED) (A)

2.3.3 Normalized Difference Built–Up Index (NDBI)

Normalized differentiated built–up index will be incorporate for extraction and identification of urban or built–up areas from imagery (Zha et al., 2003). It makes use of reflection in the near and mid–infrared wavelengths. It can be calculated as:

NDBI=(MIR–NIR)/(MIR+NIR) (B)

2.3.4 Normalized Difference Barren Index (NDBaI)

Barren lands participate an essential task in the environment and will be castoff for investigating special features of different LULC and classifying bare lands. It utilizes the reflectivity in shortwave and thermal infrared (Chen et al., 2006). It can be calculated as:

NDBaI=(SWIR–TIRS)/(SWIR+TIRS) (C)

2.3.5 Normalized Difference Water Index (NDWI)

The normalized differential index of water uses NIR and SWIR for water body study. In multiple cases, NDWI improves water competency. NDWI was established by GAO (1996) to improve the water scene feature. It can be calculated as:

NDWI=(NIR–SWIR)/(NIR+SWIR) (4)

2.4 Estimating LST from Thermal Band

To determine the land surface temperature (LST) from Landsat 5 and 7 thermal band 6 will be used for both datasets and for Landsat 8 imagery thermal band 10 and 11 will be used. It is necessary to convert the sensor measurements, which are recorded as digital numbers (DN), into a physical quantity. This can be achieved by adapting the digital numbers into additional functional real units like reflection, radiance, or temperature brightness. The subsequent approach was used to derive the LST from the thermal bands of Landsat Images. Any object with a temperature above absolute zero (0K) emits thermal electromagnetic energy, which can be detected by a thermal sensor. The data received from the thermal sensor could be exchanged to sensor level radiance using the irradiance scaling information given in satellite metadata. After this step, the spectral radiance could be extracted from data upper atmospheric temperature brightness consuming the thermal bands records offered in the metadata.

To retrieve the Earth surface temperature, a particular procedure consuming a thermal band from the data set is used. However, since the temperatures obtained with this method refer to a black body, corrections od emissivity are necessary for the Earth's surface. The emissivity can be derived from the Normalized Difference Vegetation Index (NDVI). The emissivity corrected LST is obtained using the method proposed by Artis and Carnahan (1982). The land surface emissivity is defined as the ratio of the radiated energy by a Land surface to the energy radiated by a black body at the equal temperature, wavelength, and dark conditions.

Finally, the recovered land surface temperature in Kelvin, and it could then convert to degree Celsius with the relationship of zero degrees Celsius equals to 273.15 Kelvin. The LST could be calculated by the following formula:

$$LST = Tb / [1 + (\{\lambda * Tb / p\}) * \ln(\varepsilon)] \quad (5)$$

Where Satellite temperature is Tb; wavelength of emitted radiance =w; p = h * c / s 1.438 * 10^{-2}m K; Planck's constant (h) 6.626 * 10^{-34} J s; Boltzmann Constant (s); speed of light (c) 2.998 × 10^{8} m/s; Emissivity (e). The energy radiated from a materials surface at the same temperature, wave length and viewing condition is Land surface emissivity.

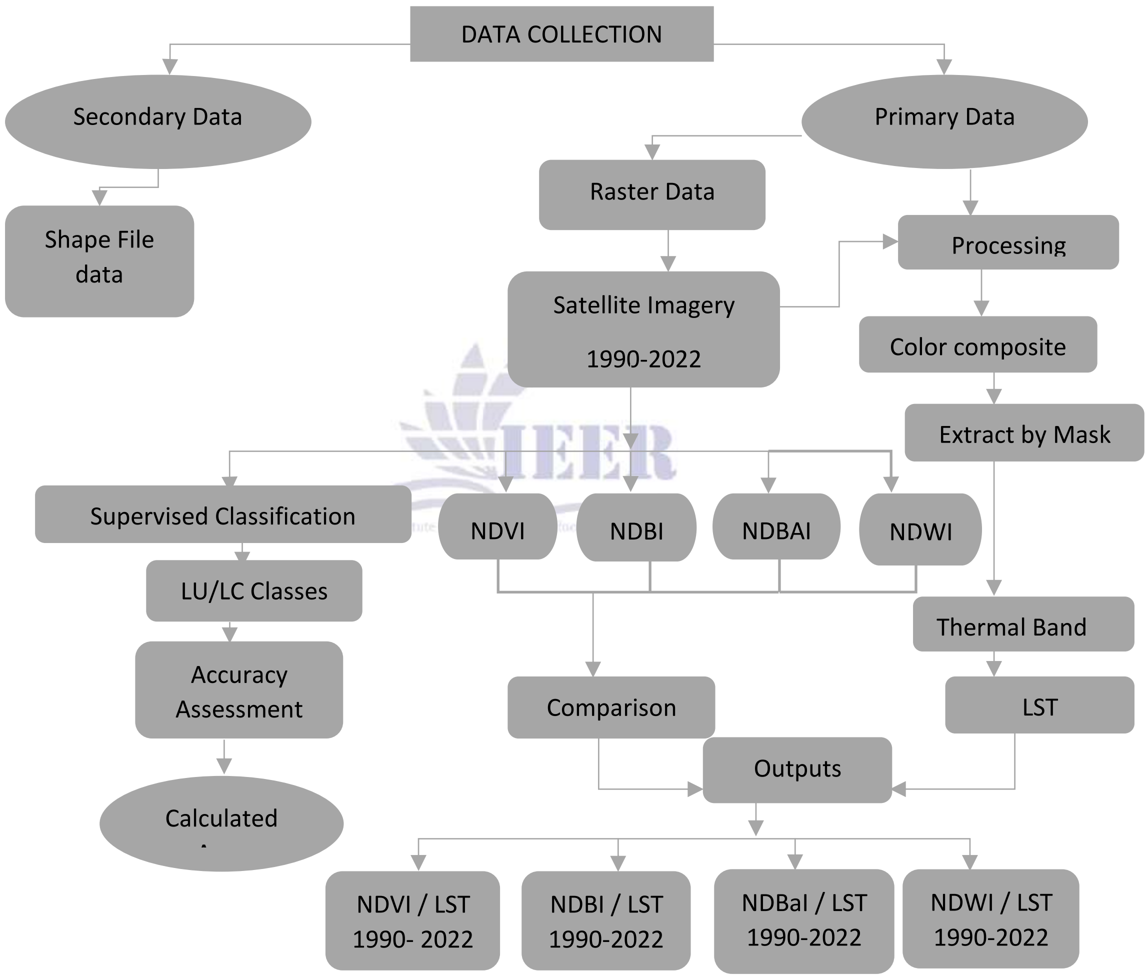

Figure 2.2 Methodological Flow Chart of Study Area

Result And Discussion

3.1 Land Use Land Cover Maps and Change Detection

A supervised maximum likelihood classification technique has been used to generate land use maps for city land cover. The total area is approximately 1,641 square kilometers. The region has been separated into five classes based on the relevance of the study: water, farmland, built–up, rocky area, and dry terrain. Multiple classes have been avoided due to the pixel mix since other classes would seize minor sections. There are found open sections, compacted dirt, and a stripped area in bare locations (Waleed *et al.*, 2020). As illustrated in Figure 3.2, 3.3, 3.4, 3.5, 3.6, 3.7, 3.8 the classed maps depict the overall outcome. The different land use classes of land cover in this area have undergone significant changes due to various types of slinked human activities. Percentage distribution of land use classes area is shown in table 3.1

Table 3.1 Land Use/Land Cover Classes area of Mardan (1990–2022)

Classes	Area Sq.km (1990)	%	Area Sq.km (2000)	%	Area Sq.km (2010)	%	Area Sq.km (2022)	%
Agriculture	838.6159	51.09851	643.086	39.1822	817.3701	49.80106	669.834	40.81192
Built Up	16.01981	0.976119	31.2984	1.906962	76.3308	4.650714	132.4539	8.070205
Barren Land	724.1749	21.56866	765.381	31.2316	869.7291	20.18958	859	19.51176
Water Body	6.321314	0.38517	6.4926	0.395584	3.1887	0.194282	1.4832	0.090369

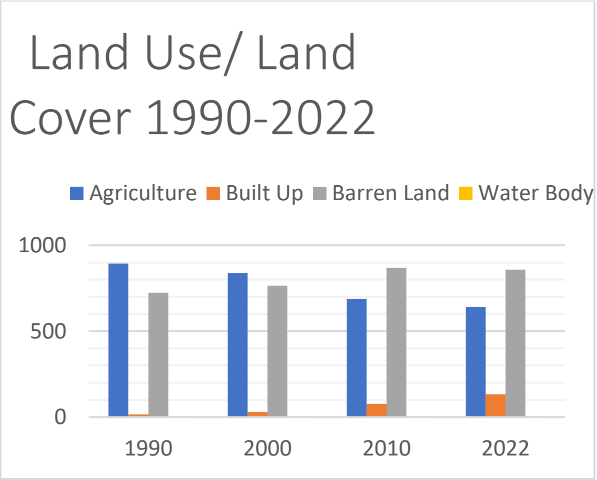

Figure 3.1 Graph of LU/LC of Mardan (1990–2022)

Due to urbanization and other human activities, agriculture, built–up regions, and dry areas have altered. activities. Agriculture area has been estimated 838, 643, 817 and 669 km² in the years 1990, 2000, 2010, and 2022 respectively. Over the past three decades, agriculture has been reduced from 51% to 40% of the total area. Agriculture area has been declined substantially in the middle of the year due to harvesting and re–cultivation in the study region, owing to the area being converted for residential and commercial usage. Since first of year of study period, the built–up area 0.97 km² in 1990, in 2000 increase to 31 km², in 2010 the built–up area increased to 76 km² and in 2022 was built up to 132 km² increased. In recent decades, development has increased from 0.97% to 8% of the total area of Mardan. The reason for this significant increase is urbanization, or the unplanned split of land use patterns, as well as industrial expansion. The barren zone shows a slight variation with 21%, 31%, 20%, and 19%. All images have been classified where the rocky area, dry land and water body in the center are slightly increased, which could occur due to the satellite resolution change from Landsat 5, 7 and

Spectrum of Engineering Sciences
ISSN (e) 3007-3138 (p) 3007-312X Volume 4, Issue 5, 2026

8, agricultural and later confirmed irregular pixels in accuracy assessment.

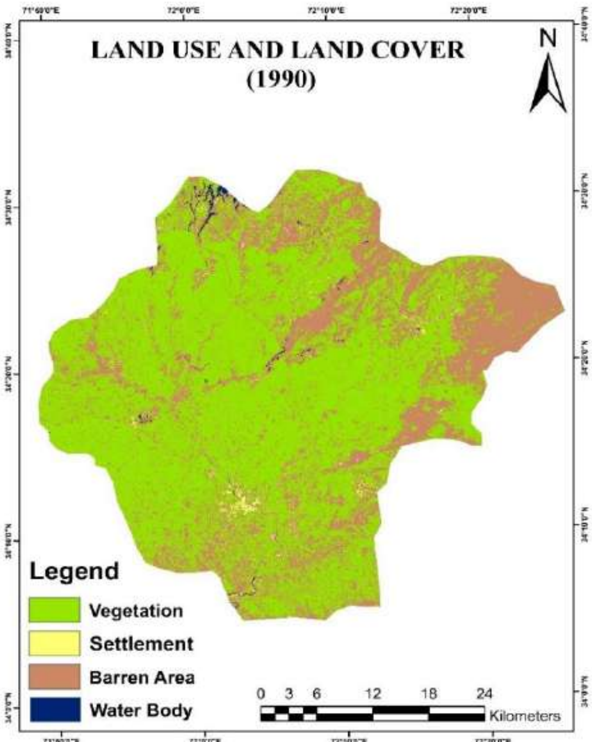

Figure 3.2 LU/LC Classes in 1990 of study area

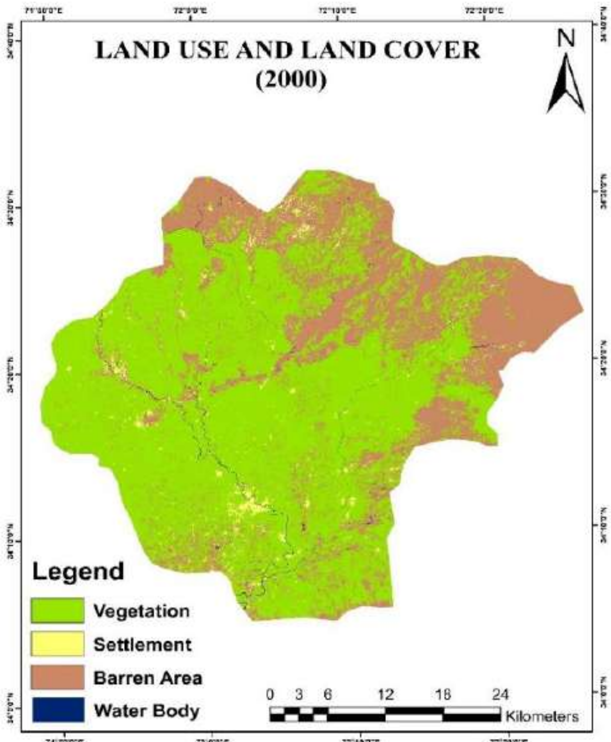

Figure 3.3 LU/LC Classes in 2000 of study area

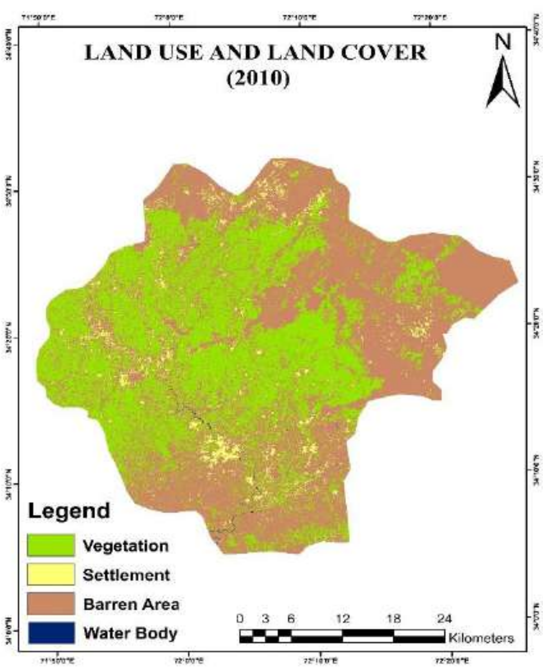

Figure 3.4 LU/LC Classes in 2010 of study area

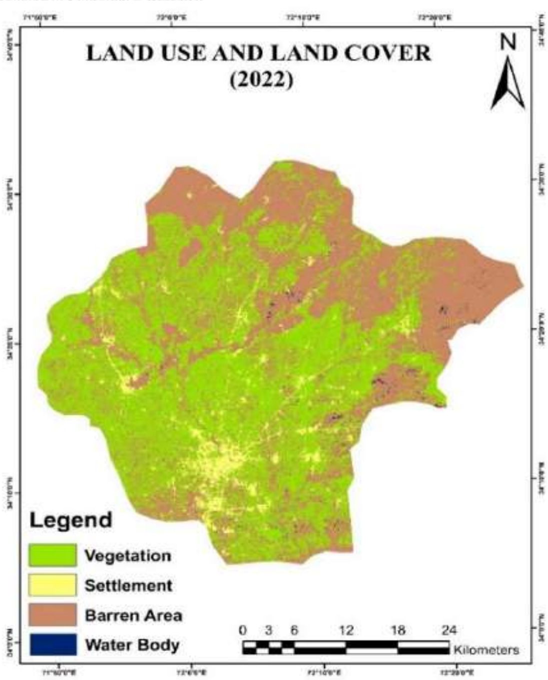

Figure 3.5 LU/LC Classes in 2022 of stud

3.2 Accuracy Assessment

To assess the accuracy of the graded images, 50 random samples have been taken from each class and a total of 250 samples from each image. Overall accuracies ranged from 0.91 for 2000, 0.90.0.91 and 0.90 for 2010, 2015, 2022 (Hugenholtz *et al.*, 2013). With kappa coefficients of 0.89, 89.0.90, 0.87, and 0.87. Table 4.2 shows kappa coefficients of 0.89, 0.89, 0.87, and 0.87. The kappa coefficient is a method for calculating a classifier's percentage improvement on a totally random set of classes. The accuracy of the result belongs to the threshold value the was assigned by many of the researcher as if the image accuracy in Kappa and Overall is higher than 0.6 then it will be considered as correct classification (Ahmed et al., 2013). The values of the results are higher than 0.6, which shows the reliability of the results.

Table 3.2 Accuracy Assessment of classified image 1990–2022

Image Years	Overall Accuracy in Percentage	Kappa coefficient
1990	0.91875	0.894137258
2000	0.912374	0.893462516
2010	0.90625	0.878524067
2022	0.90423	0.877413056

3.3 Markov Chain

To comprehend the likely change in LULC up to 2050, a transition probability picture has been constructed using the Markov chain model, as shown in Figure 3.6. Agriculture degradation and increasing in settlements provide the most potential for change in Land use– Land cover. Due to urbanization and global warming arid zones that have converted from agriculture to build up are more likely to migrate to the Land Use–Land cover model (Hamad *et al.*, 2018).

Table 3.3 Transition Probability Table

Classes	Predicted area in (2050)	Percentage of total area
Agriculture	579.856	35.32971203
Built Up	136.467	8.314719192
Barren Land	588.9546	35.88407539
Rocky Area	330.4035	20.13096443
Water Body	5.589	0.34052896

3.4 Land Surface Temperature

LST is the surface radiant skin temperature measured by a remote sensor. It is estimated from the TOA brightness temperature of the infrared channels of the satellites. It is a mixture of vegetation and bare soil temperature. Since these react quickly to incident solar radiation, changes in LST also occur rapidly. The study is based on the thermal bands calculated from the TOA brightness temperature of the Landsat satellite for each year to which a one–window algorithm has been applied to derive the LST from sensors with a single thermal band (Subzar Malik *et al.*, 2019). It uses part of the vegetation controlled by NDVI. The LST showed in numbers an increase in temperature between the specified time periods.

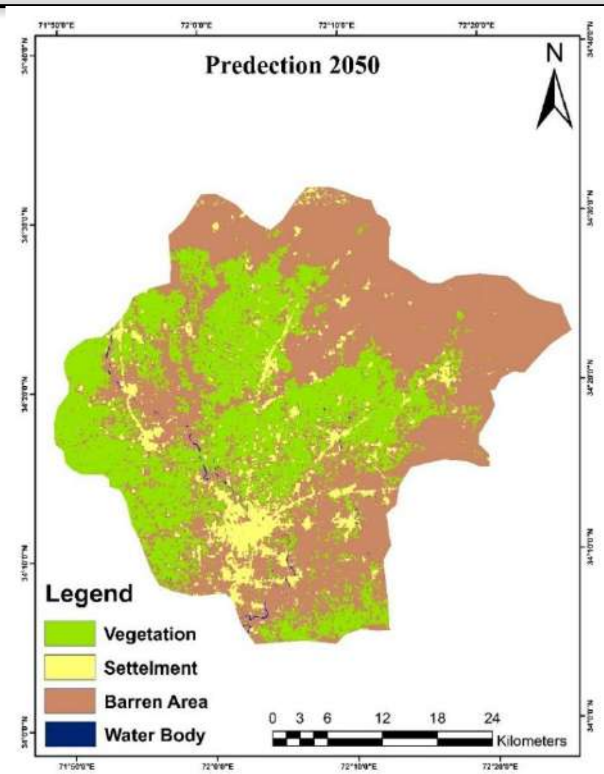

Figure 3.6 Transition Probability Map of Mardan (2050)

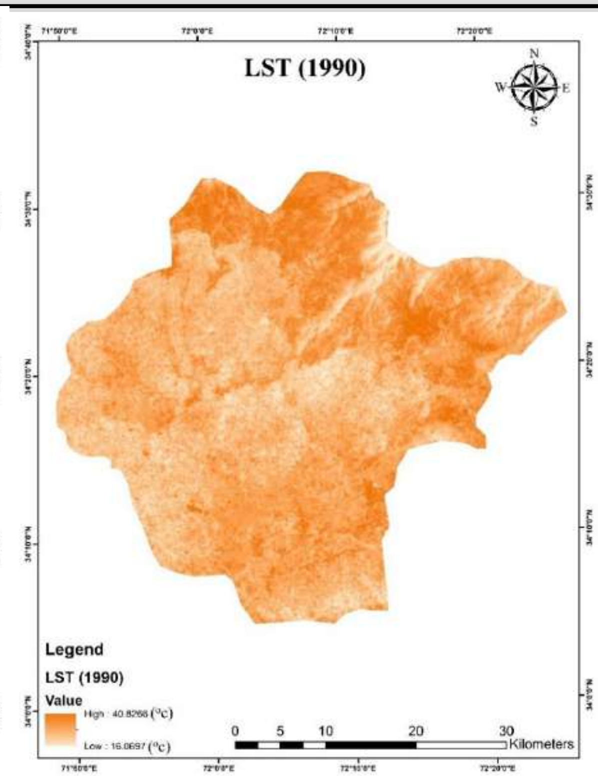

Figure 3.7 Spatial distribution of LST over Mardan in 1990

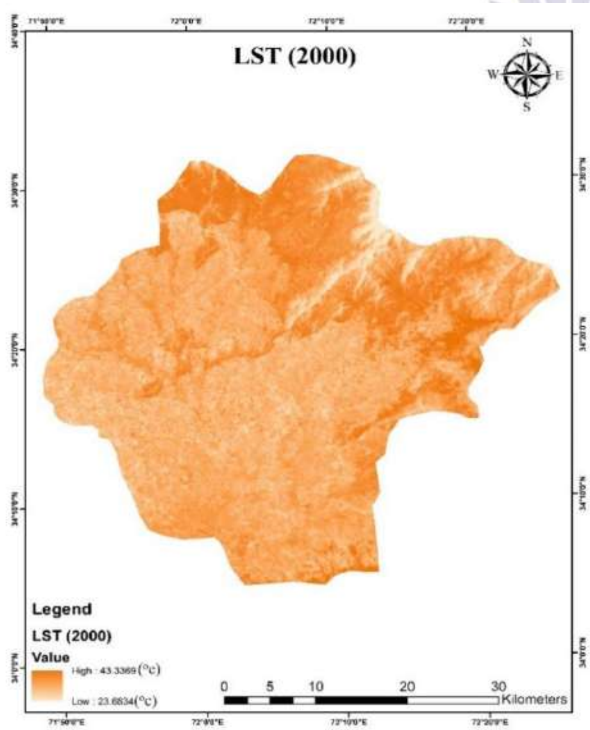

Figure 3.8 Spatial distribution of LST over Mardan in 2000

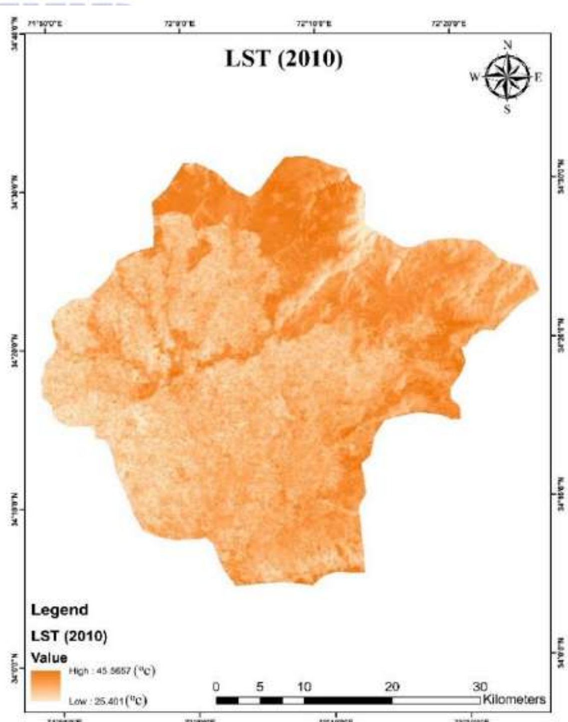

Figure 3.9 Spatial distribution of LST over Mardan in 2010

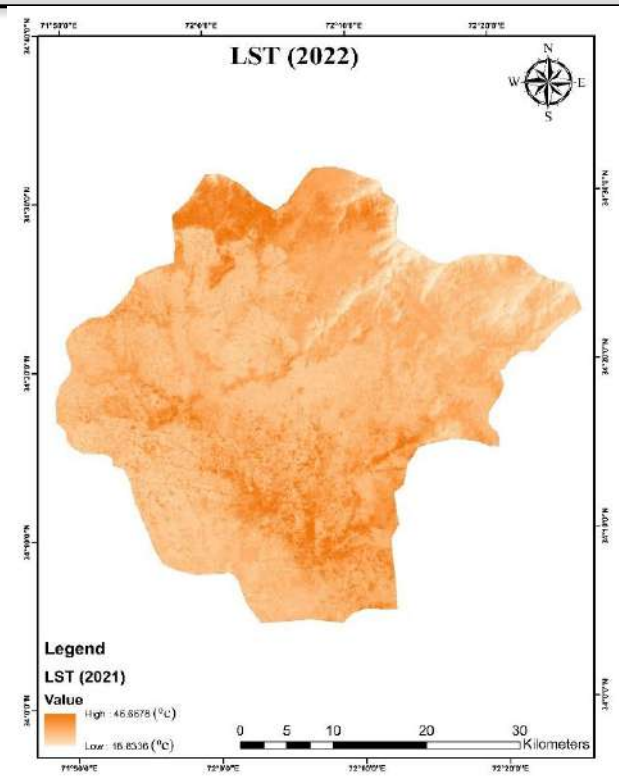

Figure 3.10 Spatial distribution of LST over Mardan in 2022

In 1990 the LST was around 40.0 C, in 2000 the LST 43.0 C was found, Moreover, in 2010, 2022 temperature of the Land area was 45, and 46.6 were determined. According to a recent study by NOAA's National Environmental Information Centers, the Earth broke the climate record by plunging the planet into the worst–case scenario, because April 2018 was the 400th consecutive month with an above average temperature, meaning 1984 was the last year. the earth had a lower temperature than normal and is heading towards the degrees Celsius of climate change (NCEI, 2017). This is also a confirmation of our study, as the temperature variation in the district on average has been 3 degrees Celsius since 1990. The LST, obtained from the latest satellite data, showed that the maximum temperature originated from urban and arid areas (34–46 ° C), as shown in the figures (from 3.10 to 3.16). Using last year's LST, regions with the highest temperature have been highlighted to collect samples of those areas and overlay them with Google Earth imagery to identify which features emit the most heat. These features have been identified as roofs, sidewalks, roads, and bare, compact soil. As these are waterproof surfaces, they are impenetrable and there is no evapotranspiration through them, trapping heat in them. Since the soil grains are not dissolved in the compacted soil, the gaps between them are small and most of the heat is retained in the soil.

3.5 NDVI and LST

The difference between the red and near infrared bands has been used to calculate the health of the vegetation using NDVI. The NDVI is calculated using the near infrared and red bands. In 1990 the NDVI value ranged from –0.52 to 0.74. In 2000 the NDVI ranged from –0.31 to 0.66, in 2010 from –0.26 to 0.56 and in 2022, it went from –0.12 to 0.45, as shown by the Figures 3.11 to 3.14. From the last 3 decades NDVI dropped due to deforestation and change of Land to Built–up area. NDVI has shown a visible shift, although a comparison with LST reveals that LST rises as vegetation cover decreases. The intensity of the LST has been impacted by the density of the vegetation. In comparison to rich plant cover, less intense plant cover is ineffective in regulating the development of intense soil surface temperature. As shown in figure 3.11 to 3.14 the maps demonstrate how vegetation density has changed throughout time. Lower NDVI values imply less vegetation cover because of urban development, whereas high NDVI values indicate dense plant cover, with a drop in vegetation density leading to an increase in temperature. Furthermore, the relation was 0.88 for 1990, 0.82 in 2000, from 2010 to 2022 0.92 and 0.71. The relation is strong in all cases, but the relationship is reversed because vegetation is strongly correlated with lower LST values, as shown in Figure 3.15.

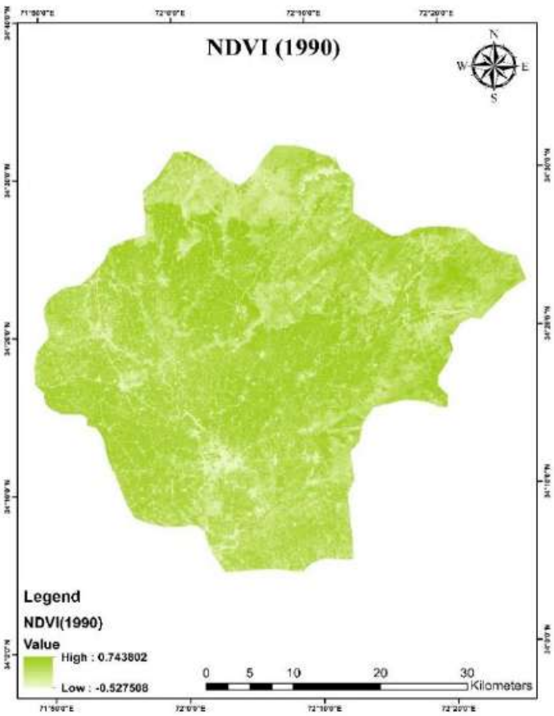

Figure 3.11 Spatial distribution of NDVI over Mardan in 1990

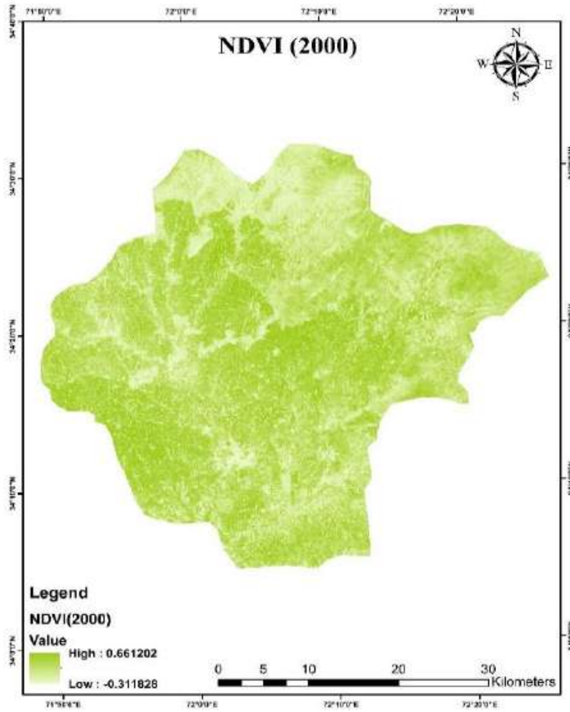

Figure 3.12 Spatial distribution of NDVI over Mardan in 2000

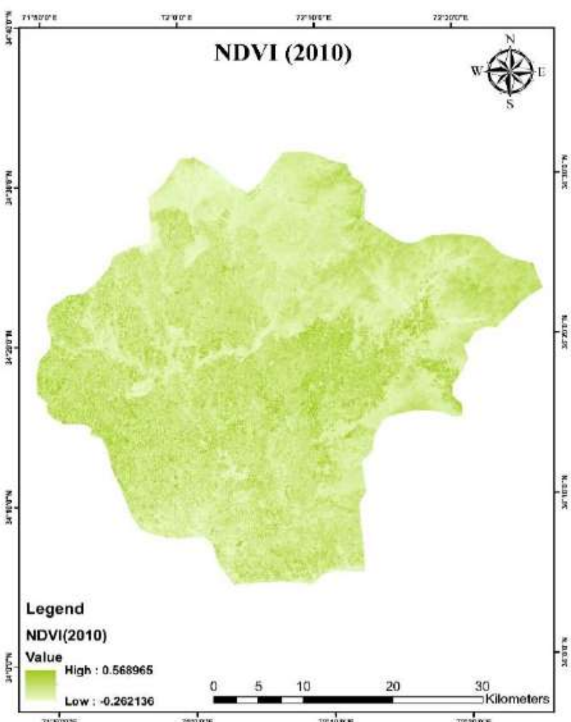

Figure 3.13 Spatial distribution of NDVI over Mardan in 2010

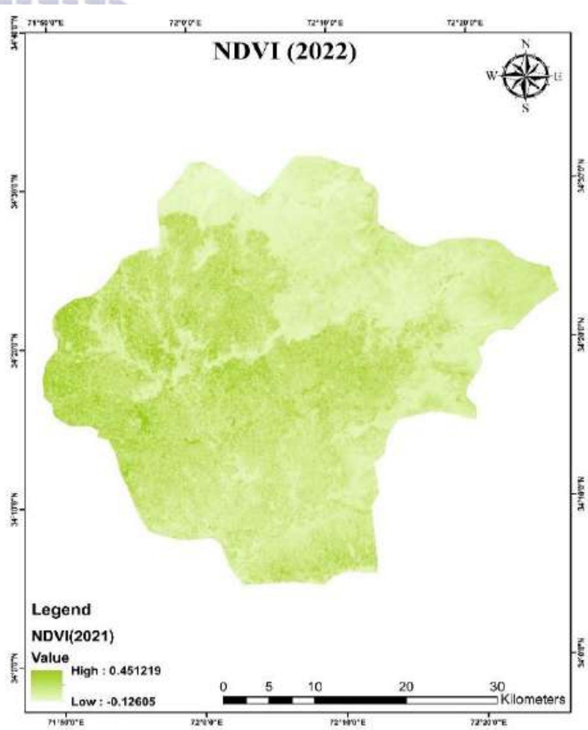

Figure 3.14 Spatial distribution of NDVI over Mardan in 2022

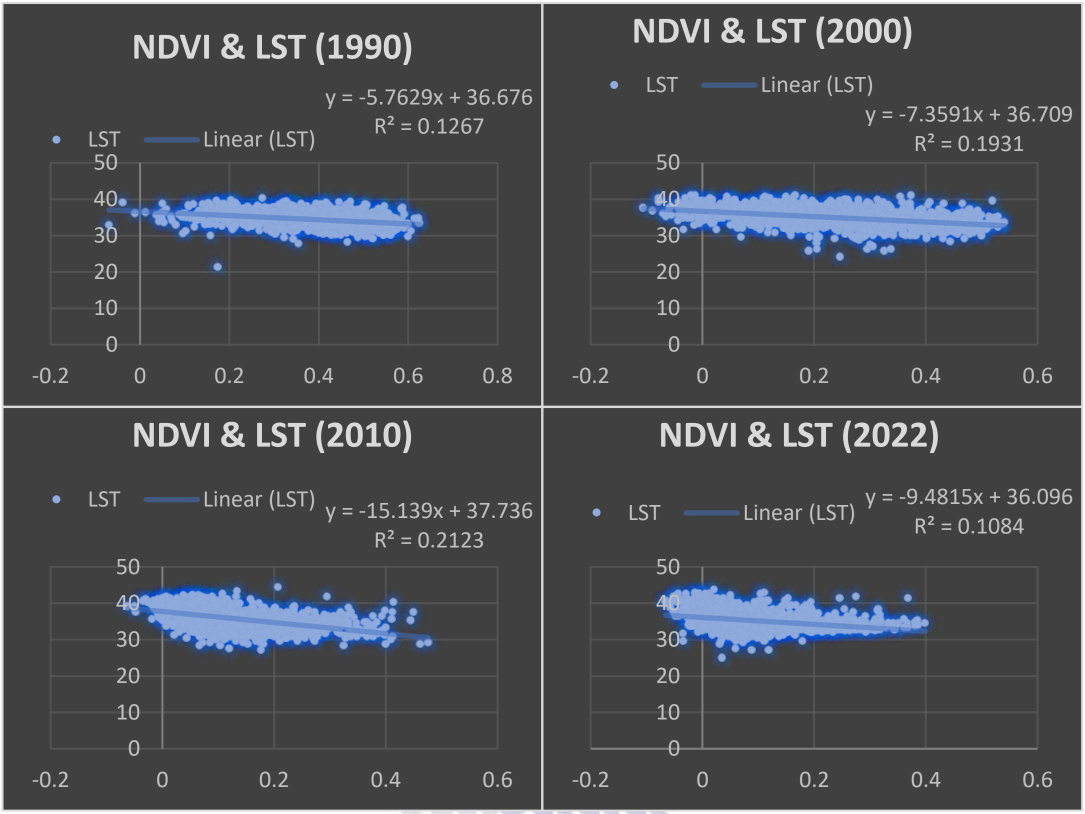

Figure 3.15 Graphs Show Relationship between NDVI and LST (1990–2022)

3.6 NDBI and LST

To extract the built area from urban land use and to intensify built up information, the normalized difference built up index is utilized. The presence of high NDBI values indicates a densely populated area. In 1990 the values ranged from –0.32 to 0.20, in 2000 from –0.38 to 0.31 and from –0.14 to 0.36, in 2010 the NDBI ranged from, –0.51 to 0.40, and in 2022, the NDBI ranged from –0.49 to 0.62. The NDBI value was growing time to time in some area the vegetation area was disturb of increasing fast growing built up. The built–up area is visible on the maps in Figures 3.16 to 3.19. A comparison between LST and NDBI shows that the soil surface temperature increases with increasing built–up area. This is because the inhabited centers are mostly made up of impermeable areas. Because the populated regions are primarily made up of impermeable zones, this is the case. Urban regions consume a lot of energy in comparison to rural places, which is why they generate a lot of heat. As the built–up area grows, excessive energy use and trapped heat become a source of high temperatures.

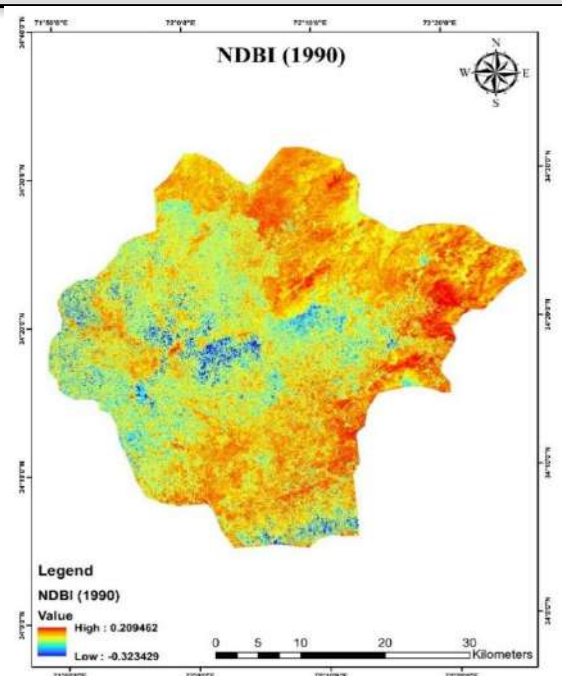

Figure 3.16 Spatial distribution of NDBI over Mardan in 1990,

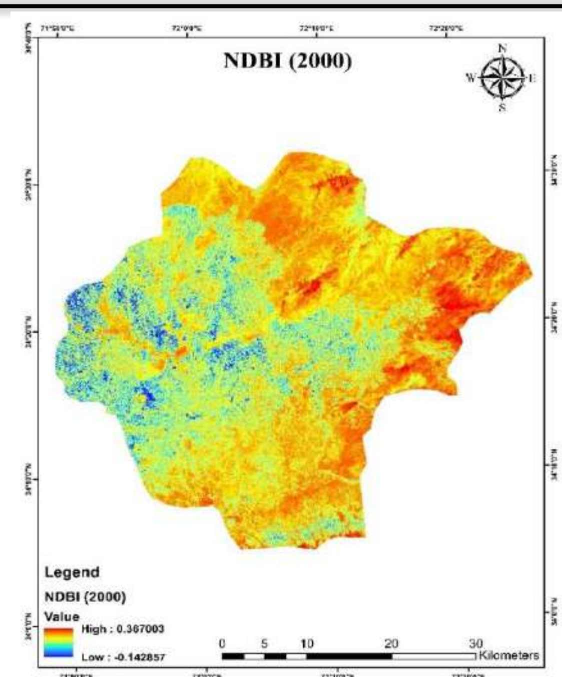

Figure 3.17 Spatial distribution of NDBI over Mardan in 2000

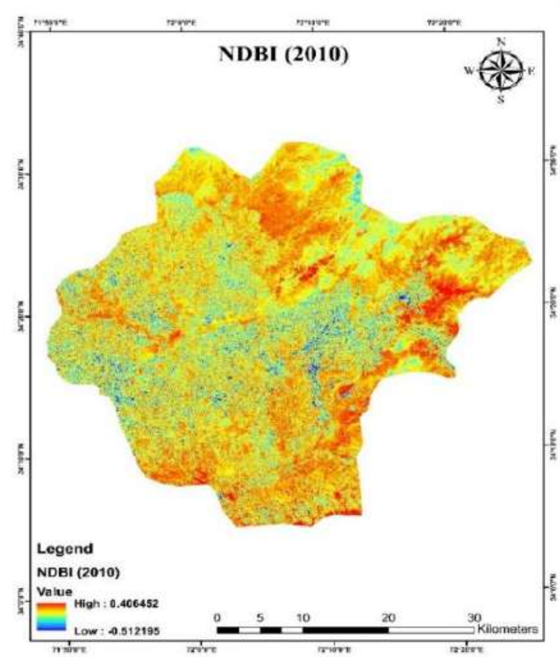

Figure 3.18 Spatial Distribution of NDBI over Mardan in 2010

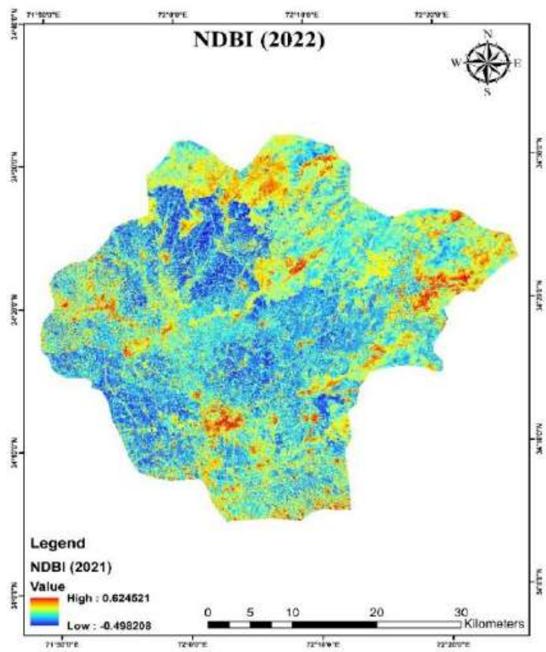

Figure 3.19 Spatial distribution of NDBI over Mardan in 2022

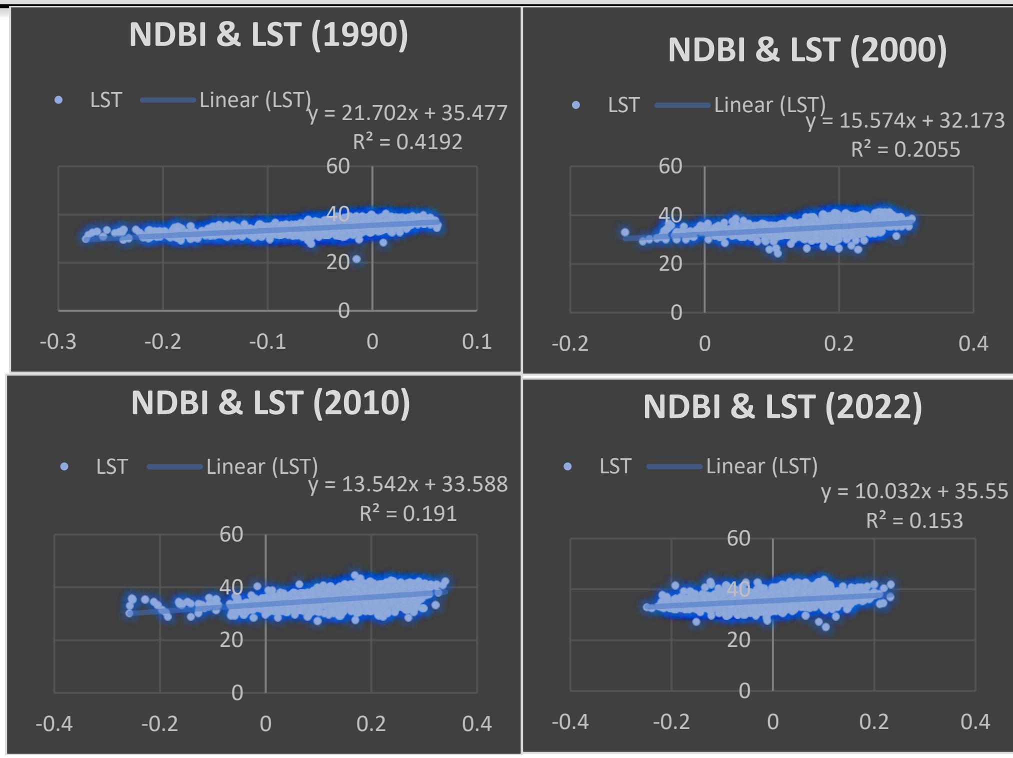

Figure 3.20 Graphs Show Relationship between of NDBI and LST (1990–2022)

The NDBI and LST have a positive relationship, indicating that the earth's surface temperature has risen as the built–up area has grown. As indicated in Figure 3.20, in 1990 the relation was 0.91 for 1995 to 0.90, in 2000 it was 0.99 for 2010, and 2022 it was –0.97. The strong the relation between the NDBI and LST, As the NDBI is increased the LST of the area were also increased. Urban environments, in comparison to rural ones, have an impermeable surface and consume a lot of energy. High temperatures might arise as a result of the increased built–up area, due to the high energy demand and massive stored heat.

3.7 NDBaI and LST

In 1990 NDBaI values ranged from –0.72 to 0.05, in 2000 from –0.69 to 0.07, in 2010 0.1, –0.84 to 0.25; NDBaI also ranged from 0.49 to 0.21 in 2022. This means that baren areas have undergone changes since 1990, as shown in Figures 3.21 to 3.24. When comparing LST to NDBaI, it's clear that as the barren zone grows, so does the LST. Due to the bigger surface area and unlimited soil particles, barren places emit heat fast and ability to retain water.

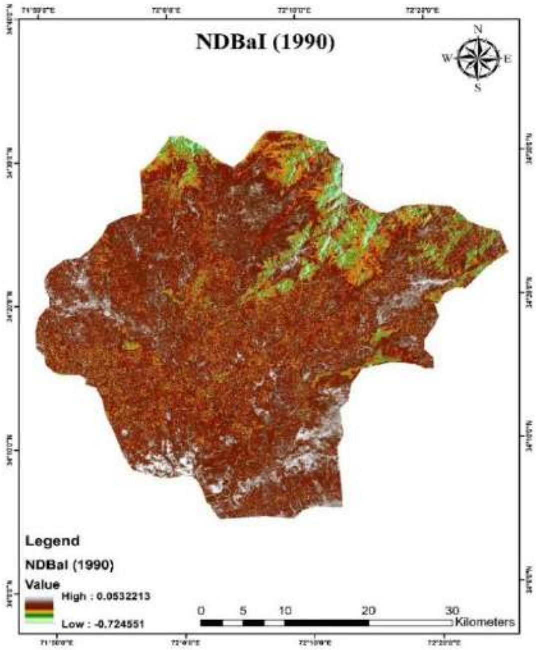

Figure 3.21 Spatial distribution of NDBaI over Mardan in 1990

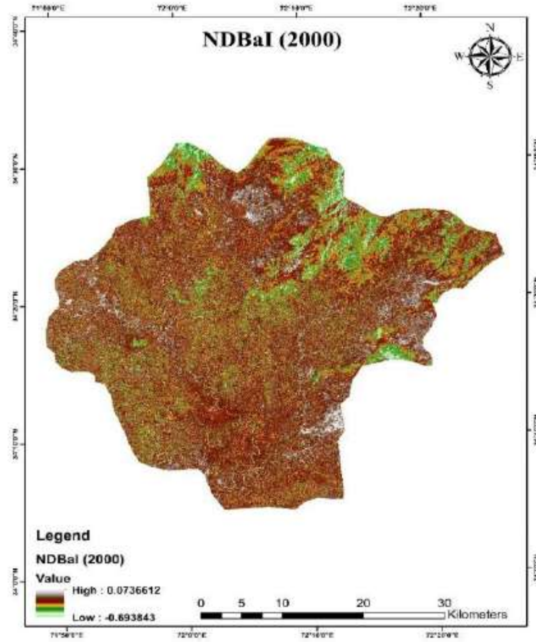

Figure 3.22 Spatial distribution of NDBaI over Mardan in 2000

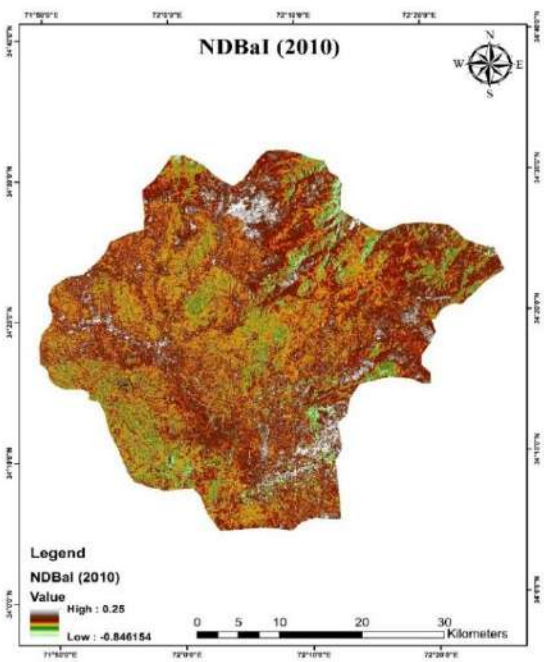

Figure 3.23 Spatial distribution of NDBaI over Mardan in 2010

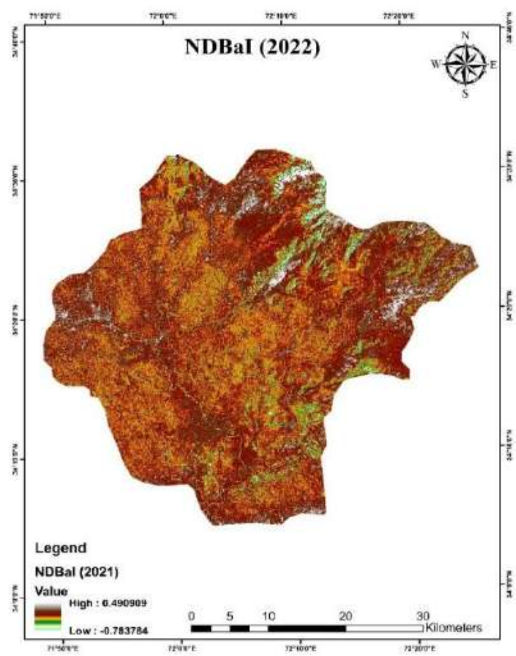

Figure 3.24 Spatial distribution of NDBaI over Mardan in 2022

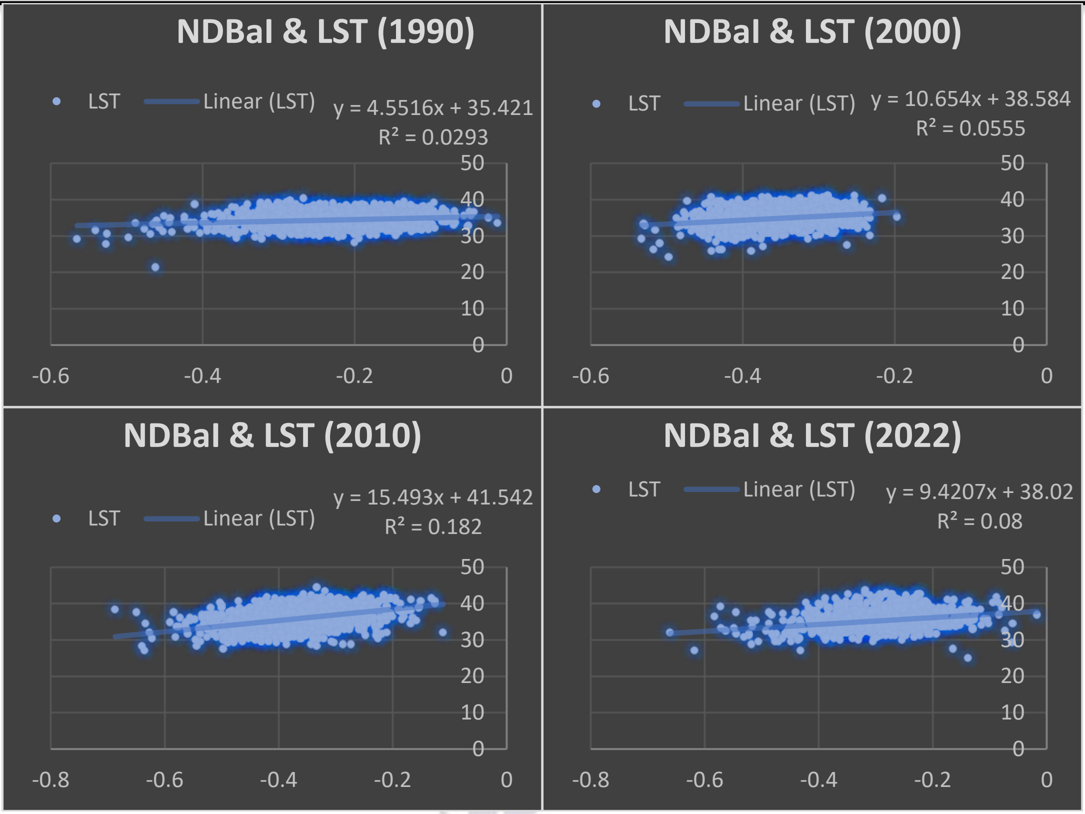

Figure 3.25 Graphs Show Relationship between NDBaI and LST (1990–2022)

There is a strong positive relationship between NDBaI and LST, which explains that the larger the sterile zone, the greater the LST. In 1990, 2000, the correlation was 0.96, 0.97, for 2010, and 0.79, in 2022 it was 0.96, as shown in figure 3.25, with a larger sterile area, because in arid areas the sand particles do not compact and a large surface has the property of releasing heat quickly, while on the other hand arid areas that have solidified and contain moisture , soils due to the accumulation of heat tend to have the ability to store heat longer.

3.8 NDWI and LST

The NDWI method is used to measure the amount of liquid water molecules in vegetation that come into contact with sun light. In 1990, 2000 NDWI values ranged from −0.41 to 0.71, from −0.62 to 0.49, 2010 from −0.20 to 0.32 and in 2022 −0.36 to 0.14 as shown in figure 3.26. The correlation between NDWI and LST is strongly positive in 1990, 2000, the correlation value was 0.86, 0.68, while in 2010 the value was 0.75. In 2022 NDWI correlation value was between 0.89. compensation, 0.69. As shown in Figure 3.31.

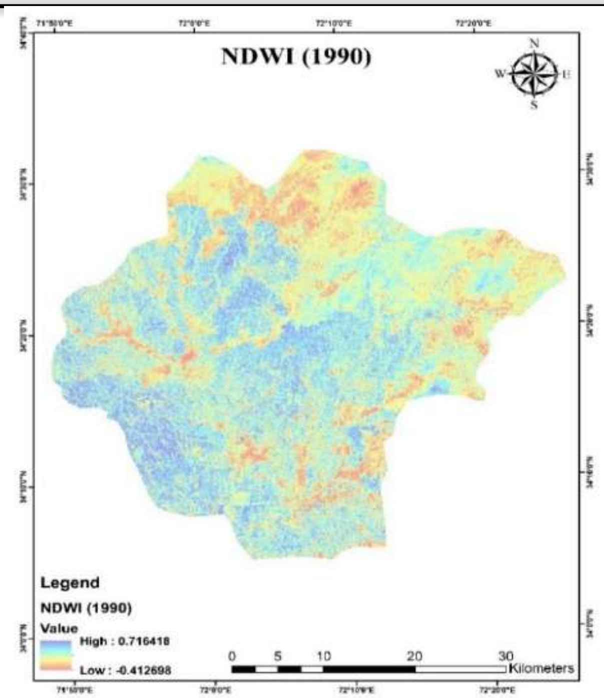

Figure 3.26 Spatial distribution of NDWI over Mardan in 1990

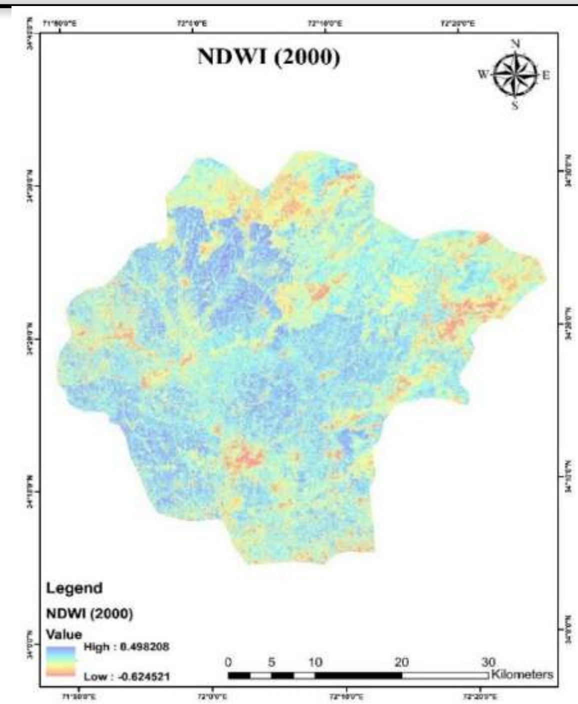

Figure 3.27 Spatial distribution of NDWI over Mardan in 2000

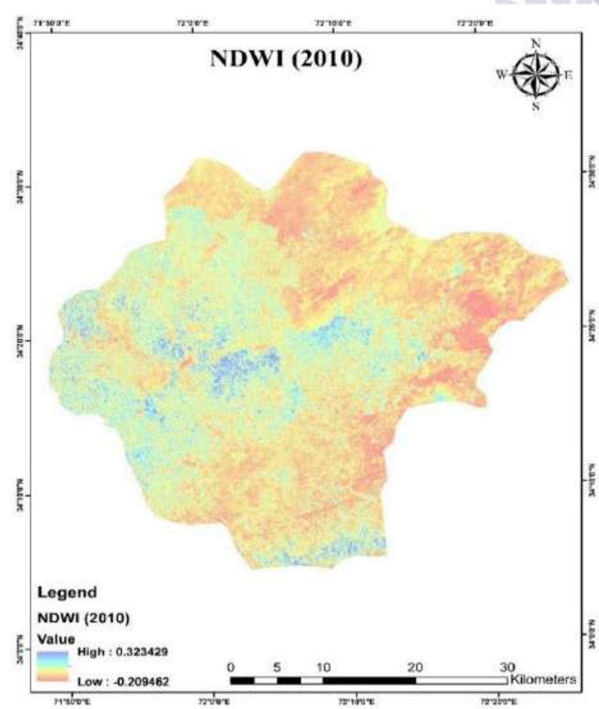

Figure 3.28 Spatial distribution of NDWI over Mardan in 2010

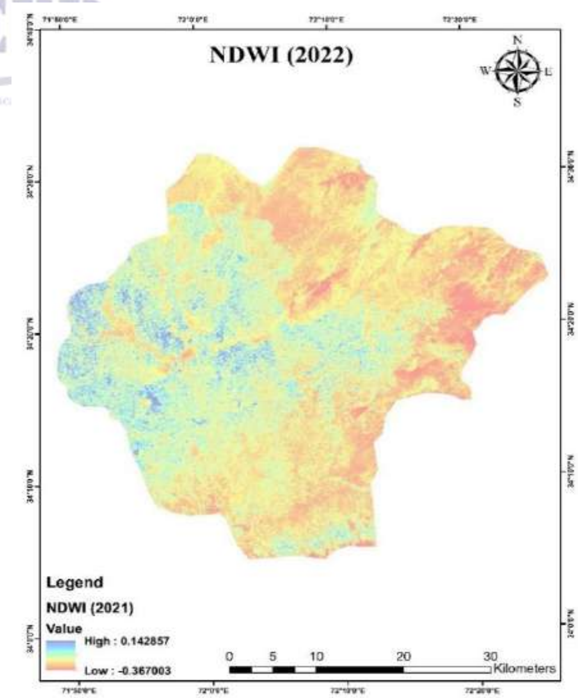

Figure 3.29 Spatial distribution of NDWI over Mardan in 2022

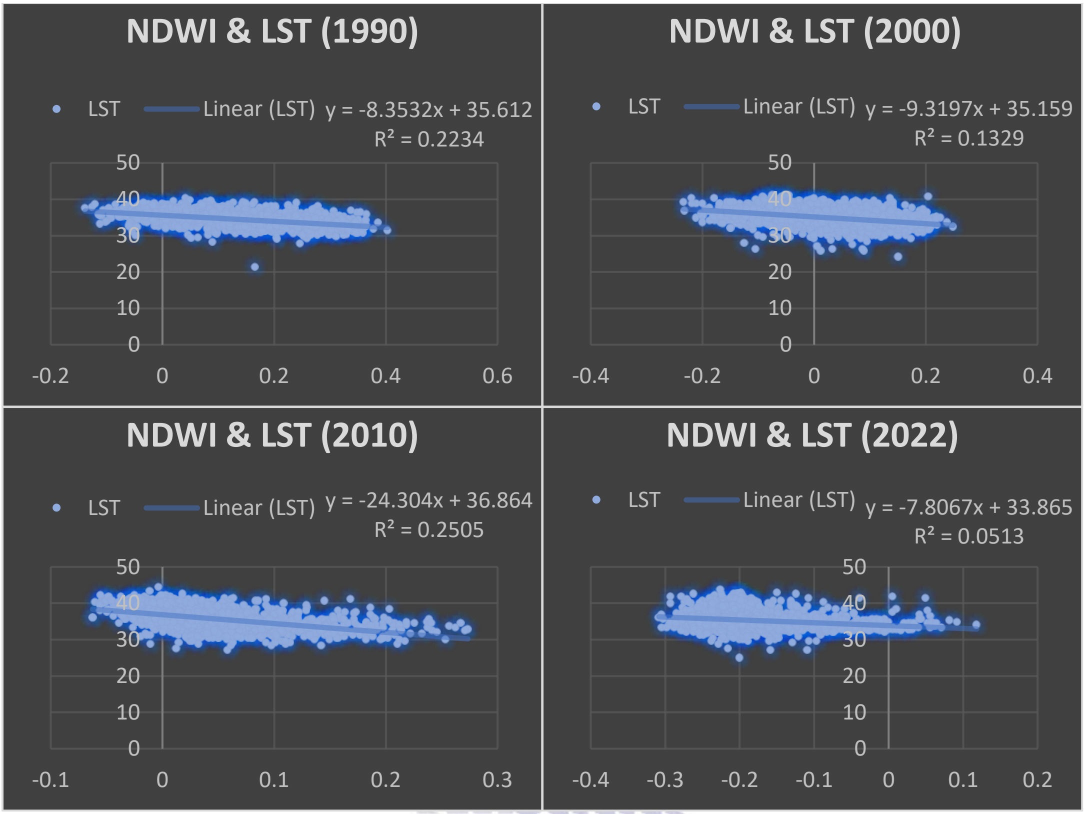

Figure 3.30 Graphs Show Relationship between NDWI and LST (1990–2022)

3.9 Urban Index (UI) and LST

The Urban Transformation Index is a measure of the impermeable areas that increased from 1990 to 2022, as shown in Figures 3.31 to 3.34. UI values ranged from −0.54 to 0.20, −0.49 to 0.24, –−0 .8 to .30, and from −0.89 to 0.49. The values showed a gradual increase showing an increase in the area under the waterproof surfaces in the last decades Shown in the picture (3.31 −3.34). UI and LST showed a strong positive relationship. This means that an increase in the user interface means an increase in LST. For the correlation, the correlation for 1990, 2000, was 0.96, 0.97, for 2010, 2022 it was 0.98, and 0.98. The correlation between waterproof surfaces and LST is strongly positive. They have a directly proportional relationship. As the seal increases, the temperature also increases, as water cannot penetrate through the sealed surfaces and therefore no evaporation or evaporation can occur. Most of the time, water flows into it. The lack of shade from the trees also contributes to this. The relationship is illustrated in Figure 3.35.

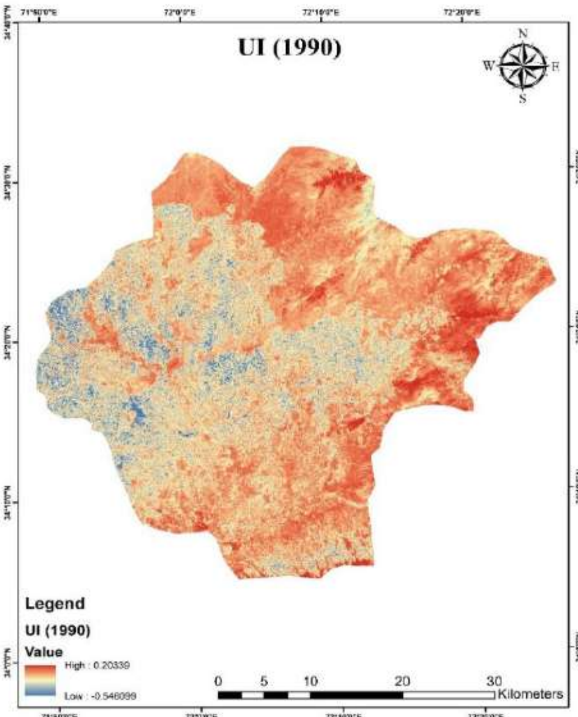

Figure 3.31 Spatial distribution of UI over Mardan in 1990

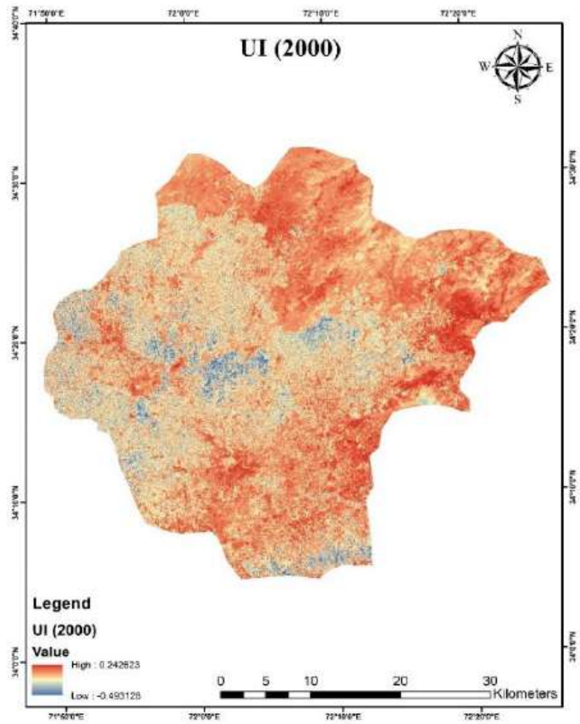

Figure 3.32 Spatial distribution of UI over Mardan in 2000

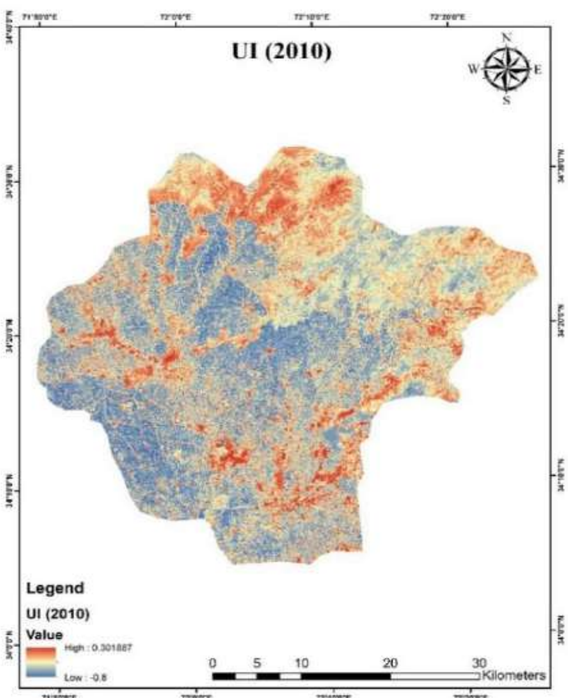

Figure 3.33 Spatial distribution of UI over Mardan in 2010

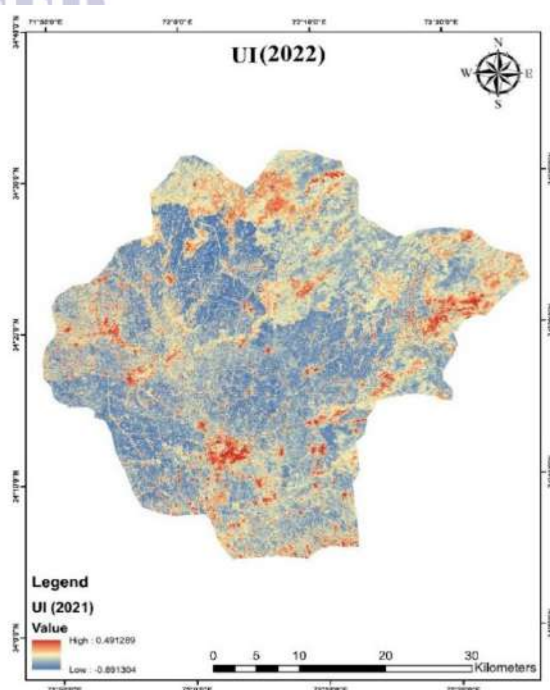

Figure 3.34 Spatial distribution of UI over Mardan in 2022

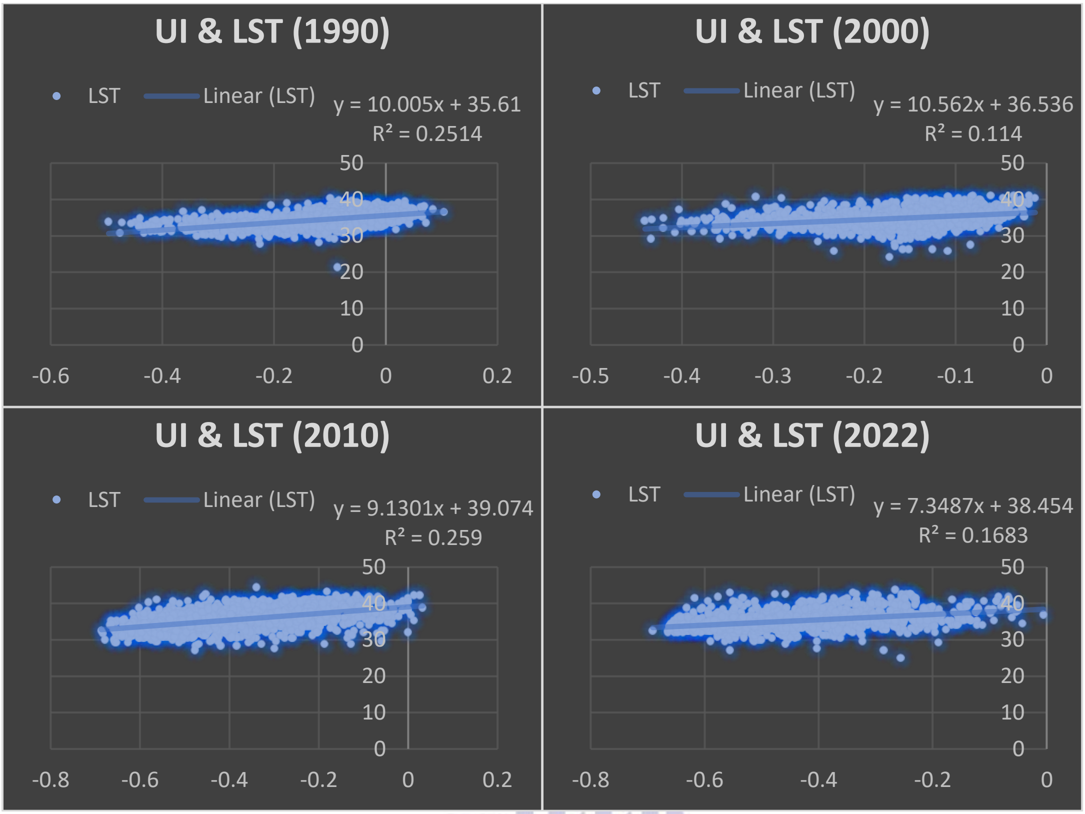

Figure 3.35 Graphs Show Relationship between UI and LST (1990–2022)

4.1 Conclusion

The generally low cost and often the availability of free low to high resolution satellite images make it an attractive way to obtain information on various environmental and climatic variables which made it possible to conduct research on a global scale. It may not be as accurate as field data, but it is certainly effective compared to field data, which is expensive and time-consuming to collect. The final note of our research is the fact that changes in a region's LULC affect that region's LST. With an increase in urban areas and a decrease in water bodies and changes in agriculture, the LST would also increase, and vice versa. Vegetation density also affects the LST of this region. Less dense vegetation means more LST as more heat is absorbed by surfaces due to reduced shade and less heat escapes through evaporation. The increase in vegetation observed in our study is due to government initiatives to control global warming. On the other hand, arid zones play the role of moderator, where they absorb heat faster than other variables, they also lose this heat quickly, but the escaping heat is captured and absorbed by buildings and thus contributes to UHI.

Such climate change has the greatest impact on a region's biodiversity, as it reacts extremely sensitively to minor changes and hinders the possibilities for adaptation. Roofs, streets, and roads are all impermeable surfaces. They are impenetrable materials, so evaporation cannot happen through them, and heat is trapped. All these surfaces raise the temperature of an area. LST and near-surface air temperature has different physical meanings and responses to atmospheric conditions, but there is a close relationship between them. The heat given off by the surface heats the air near the surface. Create a heat bubble around that region. There is usually a difference of a few degrees between them, but with complex soils this difference increases.

Brownfields, agriculture, and built-up areas are more likely to undergo a transition as the world's population grows rapidly and people seek readily available comfort and facilities in urban areas. This may require the use of vacant land suitable for conversion to urban areas. Such transitions can also affect agriculture and water. It is the age of humanity, and everyone longs for a better life, but the choices made in pursuit of a better life have profound consequences. If this trend continues, it could destroy our environment and worsen our climate. Cutting of trees and the uncontrolled and unplanned expansion of urbanization would destroy all our natural resources. Several weather services have already predicted extreme heat intensities for the future.

While the other part of the world is on the verge of freezing due to intense cold due to growing environmental imbalances. The changes may be small, but their effects will be detrimental in the long run. To control this situation, controlled urban planning and the conservation of trees and natural resources are urgently needed to correct environmental imbalances, because like our study and many other environmental and climate studies they conclude that climate change is very real and quick work.

REFERENCES

Afshan, K., Fortes-Lima, C.A., Artigas, P., Valero, M.A., Qayyum, M. and Mas-Coma, S. (no date) *Impact of climate change and man-made irrigation systems on the transmission risk, long-term trend and seasonality of human and animal fascioliasis in Pakistan*.

Amin, N.U., Hussain, A., Alamzeb, S. and Begum, S. (2013) Accumulation of heavy metals in edible parts of vegetables irrigated with waste water and their daily intake to adults and children, District Mardan, Pakistan. *Food Chemistry*, 136(3-4), 1515-1523.

Basanna, R. and Time Guest Faculty, F. (2013) *Supervised Classification for LULC Change Analysis*. 975-8887 pp.

Chakraborty, S.D., Kant, Y. and Mitra, D. (2015) Assessment of land surface temperature and heat fluxes over Delhi using remote sensing data. *Journal of Environmental Management*, 148, 143-152. Academic Press.

Estoque, R.C., Murayama, Y. and Myint, S.W. (2017) Effects of landscape composition and pattern on land surface temperature: An urban heat island study in the megacities of Southeast Asia. *Science of the Total Environment*, 577, 349-359. Elsevier B.V.

Franco, S., Mandla, V.R., Ram, K., Rao, M., Kumar, M.P. and Anand, P.C. (no date) Celso Augusto Guimarães Santos STUDY OF TEMPERATURE PROFILE ON VARIOUS LAND USE AND LAND COVER FOR EMERGING HEAT ISLAND. *Journal of Urban and Environmental Engineering*, 9(1), 32-37.

Fu, P. and Weng, Q. (2018) Variability in annual temperature cycle in the urban areas of the United States as revealed by MODIS imagery. *ISPRS Journal of Photogrammetry and Remote Sensing*, 146, 65-73. Elsevier B.V.

Hamad, R., Balzter, H. and Kolo, K. (2018) Predicting land use/land cover changes using a CA-Markov model under two different scenarios. *Sustainability (Switzerland)*, 10(10). MDPI.

Hassan, T., Zhang, J., Prodhan, F.A., Pangali Sharma, T.P. and Bashir, B. (2022) Surface urban heat islands dynamics in response to lulc and vegetation across south asia (2000-2019). *Remote Sensing*, 13(16). MDPI AG.

Hassan, Z., Shabbir, R., Ahmad, S.S., Malik, A.H., Aziz, N., Butt, A. and Erum, S. (2016a) Dynamics of land use and land cover change (LULCC) using geospatial techniques: a case study of Islamabad Pakistan. *SpringerPlus*, 5(1). SpringerOpen.

Hassan, Z., Shabbir, R., Ahmad, S.S., Malik, A.H., Aziz, N., Butt, A. and Erum, S. (2016b) Dynamics of land use and land cover change (LULCC) using geospatial techniques: a case study of Islamabad Pakistan. *SpringerPlus*, 5(1). Springer Open.

Hepcan, S., Hepcan, C.C., Kilicaslan, C., Ozkan, M.B. and Kocan, N. (2013) Analyzing landscape change and urban sprawl in a mediterranean coastal landscape: A case study from Izmir, Turkey. *Journal of Coastal Research*, 29(2), 301–310.

"Hiring of Services of Consulting Firm to Carry out Third Party Verification/validation of Pakistan 6th Population & Housing Census-2017." (2017) .

Hugenholtz, C.H., Whitehead, K., Brown, O.W., Barchyn, T.E., Moorman, B.J., LeClair, A., Riddell, K. and Hamilton, T. (2013) Geomorphological mapping with a small unmanned aircraft system (sUAS): Feature detection and accuracy assessment of a photogrammetrically-derived digital terrain model. *Geomorphology*, 194, 16–24.

Ibrahim, G.R.F. (2017) Urban land use land cover changes and their effect on land surface temperature: Case study using Dohuk City in the Kurdistan Region of Iraq. *Climate*, 5(1). MDPI AG.

Imhoff, M.L., Zhang, P., Wolfe, R.E. and Bounoua, L. (2010) Remote sensing of the urban heat island effect across biomes in the continental USA. *Remote Sensing of Environment*, 114(3), 504–513.

Jimenez-Munoz, J.C., Sobrino, J.A., Skokovic, D., Mattar, C. and Cristobal, J. (2014) Land surface temperature retrieval methods from landsat-8 thermal infrared sensor data. *IEEE Geoscience and Remote Sensing Letters*, 11(10), 1840–1843. Institute of Electrical and Electronics Engineers Inc.

Kabisch, N., Selsam, P., Kirsten, T., Lausch, A. and Bumberger, J. (2019) A multi-sensor and multi-temporal remote sensing approach to detect land cover change dynamics in heterogeneous urban landscapes. *Ecological Indicators*, 99, 273–282. Elsevier B.V.

Khan, A.A., Najam Ul Hassan, S., Baig, S., Khan, M.Z. and Muhammad, A. (2019) *The Response of Land Surface Temperature to the Changing Land-Use Land-Cover in a Mountainous Landscape under the Influence of Urbanization: Gilgit City as a case study in the Hindu Kush Himalayan Region of Pakistan*. 40–49 pp.

Khan, M.S., Ullah, S., Sun, T., Rehman, A.U. and Chen, L. (2020) Land-use/land-cover changes and its contribution to urban heat Island: A case study of Islamabad, Pakistan. *Sustainability (Switzerland)*, 12(9). MDPI.

Lelieveld, J., Evans, J.S., Fnais, M., Giannadaki, D. and Pozzer, A. (2015) The contribution of outdoor air pollution sources to premature mortality on a global scale. *Nature*, 525(7569), 367–371. Nature Publishing Group.

Li, Z.L., Tang, B.H., Wu, H., Ren, H., Yan, G., Wan, Z., Trigo, I.F. and Sobrino, J.A. (2013) Satellite-derived land surface temperature: Current status and perspectives. *Remote Sensing of Environment*. .

Ma, Y., Kuang, Y. and Huang, N. (2010) Coupling urbanization analyses for studying urban thermal environment and its interplay with biophysical parameters based on TM/ETM+ imagery. *International Journal of Applied Earth Observation and Geoinformation*, 12(2), 110–118. Elsevier B.V.

Mehmood, H., Sajjad, S.H. and Shirazi, S.A. (2017) *SPATIO-TEMPORAL TRENDS AND PATTERNS OF URBAN SPRAWL IN GUJRANWALA CITY, PUNJAB-PAKISTAN.*

Munthali, M.G., Davis, N., Adeola, A.M. and Botai, J.O. (2020) The impacts of land use and land cover dynamics on natural resources and rural livelihoods in Dedza District, Malawi. *Geocarto International*, 1–18. Taylor and Francis Ltd.

Muster, S., Langer, M., Heim, B., Westermann, S. and Boike, J. (2012) Subpixel heterogeneity of ice-wedge polygonal tundra: A multi-scale analysis of land cover and evapotranspiration in the Lena River Delta, Siberia. *Tellus, Series B: Chemical and Physical Meteorology*, 64(1).

Powell, R.L. and Roberts, D.A. (2010) *Characterizing Urban Land-Cover Change in Rondônia, Brazil: 1985 to 2000 Author(s)*. University of Texas Press, 183–211 pp.

Qiao, C., Luo, J., Sheng, Y., Shen, Z., Zhu, Z. and Ming, D. (2012) An Adaptive Water Extraction Method from Remote Sensing Image Based on NDWI. *Journal of the Indian Society of Remote Sensing*, 40(3), 421–433.

Rahman, A., Kumar, S., Fazal, S. and Siddiqui, M.A. (2012) Assessment of Land use/land cover Change in the North-West District of Delhi Using Remote Sensing and GIS Techniques. *Journal of the Indian Society of Remote Sensing*, 40(4), 689–697.

Raziq, A., Xu, A. and Li, Y. (2016) Monitoring of Land Use/Land Cover Changes and Urban Sprawl in Peshawar City in Khyber Pakhtunkhwa: An Application of Geo-Information Techniques Using of Multi-Temporal Satellite Data. *Journal of Remote Sensing & GIS*, 05(04). OMICS Publishing Group.

Ren, C., Spit, T., Lenzholzer, S., Yim, H.L.S., van Hove, B.H., Chen, L., Kupski, S., Burghardt, R. and Katzschner, L. (2012) Urban Climate Map System for Dutch spatial planning. *International Journal of Applied Earth Observation and Geoinformation*, 18(1), 207–221. Elsevier B.V.

Şahin, M., Yildiz, B.Y., Şenkal, O. and Peştemalci, V. (2012) Modelling and Remote Sensing of Land Surface Temperature in Turkey. *Journal of the Indian Society of Remote Sensing*, 40(3), 399–409.

Shekhar, S. and Pandey, A.C. (2015) Delineation of groundwater potential zone in hard rock terrain of India using remote sensing, geographical information system (GIS) and analytic hierarchy process (AHP) techniques. *Geocarto International*, 30(4), 402–421. Taylor and Francis Ltd.

Shiferaw, A. and Singh, K.L. (2011) *Evaluating The Land Use And Land Cover Dynamics In Borena Woreda South Wollo Highlands, Ethiopia*.

Solangi, Y.A., Tan, Q., Mirjat, N.H. and Ali, S. (2019) Evaluating the strategies for sustainable energy planning in Pakistan: An integrated SWOT-AHP and Fuzzy-TOPSIS approach. *Journal of Cleaner Production*, 236. Elsevier Ltd.

Subzar Malik, M., Prakash Shukla, J. and Mishra, S. (2019) *Relationship of LST, NDBI and NDVI using Landsat-8 data in Kandaihimmat Watershed, Hoshangabad, India*. 25–31 pp.

Sundara Kumar, * K, Udaya Bhaskar, P., Padmakumari, K., Seto, K.C., Woodcock, C.E., Song, C., Huang, X., Lu, J. and Kaufmann, R.K. (no date) *ESTIMATION OF LAND SURFACE TEMPERATURE TO STUDY URBAN HEAT ISLAND EFFECT USING LANDSAT ETM+ IMAGE*.

Tan, K.C., Lim, H.S., MatJafri, M.Z. and Abdullah, K. (2010) Landsat data to evaluate urban expansion and determine land use/land cover changes in Penang Island, Malaysia. *Environmental Earth Sciences*, 60(7), 1509–1521.

Vani, M. and Prasad, P.R.C. (2020) Assessment of spatio-temporal changes in land use and land cover, urban sprawl, and land surface temperature in and around Vijayawada city, India. *Environment, Development and Sustainability*, 22(4), 3079–3095. Springer.

Vivekananda, G.N., Swathi, R. and Sujith, A.V.L.N. (2022) multi-temporal image analysis for LULC classification and change detection. *European Journal of Remote Sensing*, 54(sup2), 189–199. Taylor and Francis Ltd.

Waleed, M., Ahmad, S.R., Javed, M.A. and Samiullah, S. (2020) Identification of irrigation potential areas, using multi-criteria analysis in Khyber District, Pakistan. *Environmental Science and Pollution Research*, 27(32), 39832–39840. Springer Science and Business Media Deutschland GmbH.

Wang, Y., Du, H., Xu, Y., Lu, D., Wang, X. and Guo, Z. (2018) Temporal and spatial variation relationship and influence factors on surface urban heat island and ozone pollution in the Yangtze River Delta, China. *Science of the Total Environment*, 631–632, 921–933. Elsevier B.V.

Zhang, M. and Lin, H. (2019) Object-based rice mapping using time-series and phenological data. *Advances in Space Research*, 63(1), 190–202. Elsevier Ltd.

Zhao, L., Qiu, G., Anderson, C.W.N., Meng, B., Wang, D., Shang, L., Yan, H. and Feng, X. (2016) Mercury methylation in rice paddies and its possible controlling factors in the Hg mining area, Guizhou province, Southwest China. *Environmental Pollution*, 215, 1–9. Elsevier Ltd.